Relevant degrees of freedom for $0\nu\beta\beta$ decay nuclear matrix elements with energy density functionals

Tomás R. Rodríguez

Interfacing theory and experiment for reliable double-beta decay matrix element calculations

Vancouver, May 11-13, 2016

Outline

J. Menéndez (University of Tokio)

G. Martínez-Pinedo (TU-Darmstadt)

A. Poves (UAM-Madrid)

F. Nowacki (IPHC-Strasbourg)

J. Engel (UNC-Chapel Hill)

N. Hinohara (MSU-East Lansing)

N. López-Vaquero (UAM-Madrid)

J. L. Egido (UAM-Madrid)

Outline

1. EDF method

2. Multipole deformation

3. Pairing

4. Seniority and SU(4)

5. Summary and open questions

Nuclear Matrix Elements

- Nuclear structure methods for calculating these NME:

Different ways to deal with:
- Finding the best initial and final ground states.
- Handling the transition operator (inclusion of most relevant terms, corrections, approximations, etc.).

Some remarks about these methods:
- Calculations with limited single particle bases.
- Difficulties to include collective/single particle degrees of freedom.
- Problems with particle number/isospin conservation.

Gogny EDF

Effective nucleon-nucleon interaction: Gogny force (D1S/D1M)

$$V(1,2)=\sum_{i=1}^{2}e^{-(\vec{r}_1-\vec{r}_2)^2/\mu_i^2}\left(W_i+B_iP^\sigma-H_iP^\tau-M_iP^\sigma P^\tau\right)$$
$$+iW_0(\sigma_1+\sigma_2)\vec{k}\times\delta(\vec{r}_1-\vec{r}_2)\vec{k}+V_{\mathrm{Coulomb}}(\vec{r}_1,\vec{r}_2)$$

2-body potential

$$+t_3(1+x_0P^\sigma)\delta(\vec{r}_1-\vec{r}_2)\rho^\alpha\left((\vec{r}_1+\vec{r}_2)/2\right)$$

Density dependent term

Gogny EDF

Effective nucleon-nucleon interaction: Gogny force (D1S/D1M)

$$V(1,2)=\sum_{i=1}^{2}e^{-(\vec{r}_1-\vec{r}_2)^2/\mu_i^2}\left(W_i+B_iP^\sigma-H_iP^\tau-M_iP^\sigma P^\tau\right)$$
$$+iW_0(\sigma_1+\sigma_2)\vec{k}\times\delta(\vec{r}_1-\vec{r}_2)\vec{k}+V_{\text{Coulomb}}(\vec{r}_1,\vec{r}_2)$$

2-body potential

$$+t_3(1+x_0P^\sigma)\delta(\vec{r}_1-\vec{r}_2)\rho^\alpha\left((\vec{r}_1+\vec{r}_2)/2\right)$$

Density dependent term

Next step: Variational method!!!

EDF axial

- Initial intrinsic states: PN-VAP M. Anguiano, J. L. Egido, and L. M. Robledo, Nucl. Phys. A 696, 467 (2001).

$$E^{N,Z}[\Phi] = \frac{\langle\Phi|\hat{H}_{2\mathrm{b}}\hat{P}^{N}\hat{P}^{Z}|\Phi\rangle}{\langle\Phi|\hat{P}^{N}\hat{P}^{Z}|\Phi\rangle} + \varepsilon_{DD}^{N,Z}(\Phi) - \lambda_{q_{20}}\langle\Phi|\hat{Q}_{20}|\Phi\rangle$$

EDF axial

- Initial intrinsic states: PN-VAP M. Anguiano, J. L. Egido, and L. M. Robledo, Nucl. Phys. A 696, 467 (2001).

$$E^{N,Z}[\Phi] = \frac{\langle\Phi|\hat{H}_{2\mathrm{b}}\hat{P}^N\hat{P}^Z|\Phi\rangle}{\langle\Phi|\hat{P}^N\hat{P}^Z|\Phi\rangle} + \varepsilon^{N,Z}_{DD}(\Phi) - \lambda_{q_{20}}\langle\Phi|\hat{Q}_{20}|\Phi\rangle$$

- Intermediate Particle Number and Angular Momentum Projected states

$$|I;NZ;\beta_2\rangle = \frac{2I+1}{2}\int_0^{\pi} d^{I*}_{00}(\beta)e^{-i\beta\hat{J}_y}\hat{P}^N\hat{P}^Z|\Phi\rangle\, d\beta$$

EDF axial

1. EDF method 2. Multipole deformation 3. Pairing 4. Seniority and SU(4) 5. Summary and open questions

- Initial intrinsic states: PN-VAP M. Anguiano, J. L. Egido, and L. M. Robledo, Nucl. Phys. A 696, 467 (2001).

$$E^{N,Z}[\Phi] = \frac{\langle\Phi|\hat{H}_{2b}\hat{P}^N\hat{P}^Z|\Phi\rangle}{\langle\Phi|\hat{P}^N\hat{P}^Z|\Phi\rangle} + \varepsilon_{DD}^{N,Z}(\Phi) - \lambda_{q_{20}}\langle\Phi|\hat{Q}_{20}|\Phi\rangle$$

- Intermediate Particle Number and Angular Momentum Projected states

$$|I;NZ;\beta_2\rangle = \frac{2I+1}{2}\int_0^\pi d_{00}^{I*}(\beta)e^{-i\beta\hat{J}_y}\hat{P}^N\hat{P}^Z|\Phi\rangle\, d\beta$$

- Final GCM states $|I;NZ;\sigma\rangle = \sum_{\beta_2} f_{\beta_2}^{I;NZ;\sigma}|I;NZ;\beta_2\rangle$

EDF axial

- Initial intrinsic states: PN-VAP M. Anguiano, J. L. Egido, and L. M. Robledo, Nucl. Phys. A 696, 467 (2001).

$$E^{N,Z}[\Phi] = \frac{\langle\Phi|\hat{H}_{2b}\hat{P}^N\hat{P}^Z|\Phi\rangle}{\langle\Phi|\hat{P}^N\hat{P}^Z|\Phi\rangle} + \varepsilon_{DD}^{N,Z}(\Phi) - \lambda_{q_{20}}\langle\Phi|\hat{Q}_{20}|\Phi\rangle$$

- Intermediate Particle Number and Angular Momentum Projected states

$$|I;NZ;\beta_2\rangle = \frac{2I+1}{2}\int_0^{\pi} d_{00}^{I*}(\beta)e^{-i\beta\hat{J}_y}\hat{P}^N\hat{P}^Z|\Phi\rangle\, d\beta$$

- Final GCM states $|I;NZ;\sigma\rangle = \sum_{\beta_2} f_{\beta_2}^{I;NZ;\sigma}|I;NZ;\beta_2\rangle$

$$\sum_{\beta_2'}\left(\mathcal{H}_{\beta_2,\beta_2'}^{I;NZ} - E^{I;NZ;\sigma}\mathcal{N}_{\beta_2,\beta_2'}^{I;NZ}\right) f_{\beta_2'}^{I;NZ;\sigma} = 0$$

$$\mathcal{N}_{\beta_2,\beta_2'}^{I;NZ} = \langle I;NZ;\beta_2|I;NZ;\beta_2'\rangle$$

$$\mathcal{H}_{\beta_2,\beta_2'}^{I;NZ} = \langle I;NZ;\beta_2|\hat{H}_{2b}|I;NZ;\beta_2'\rangle + \varepsilon_{DD}^{I;NZ}\left(\Phi(\beta_2),\Phi(\beta_2')\right)$$

EDF axial

Determination of initial and final states (I)

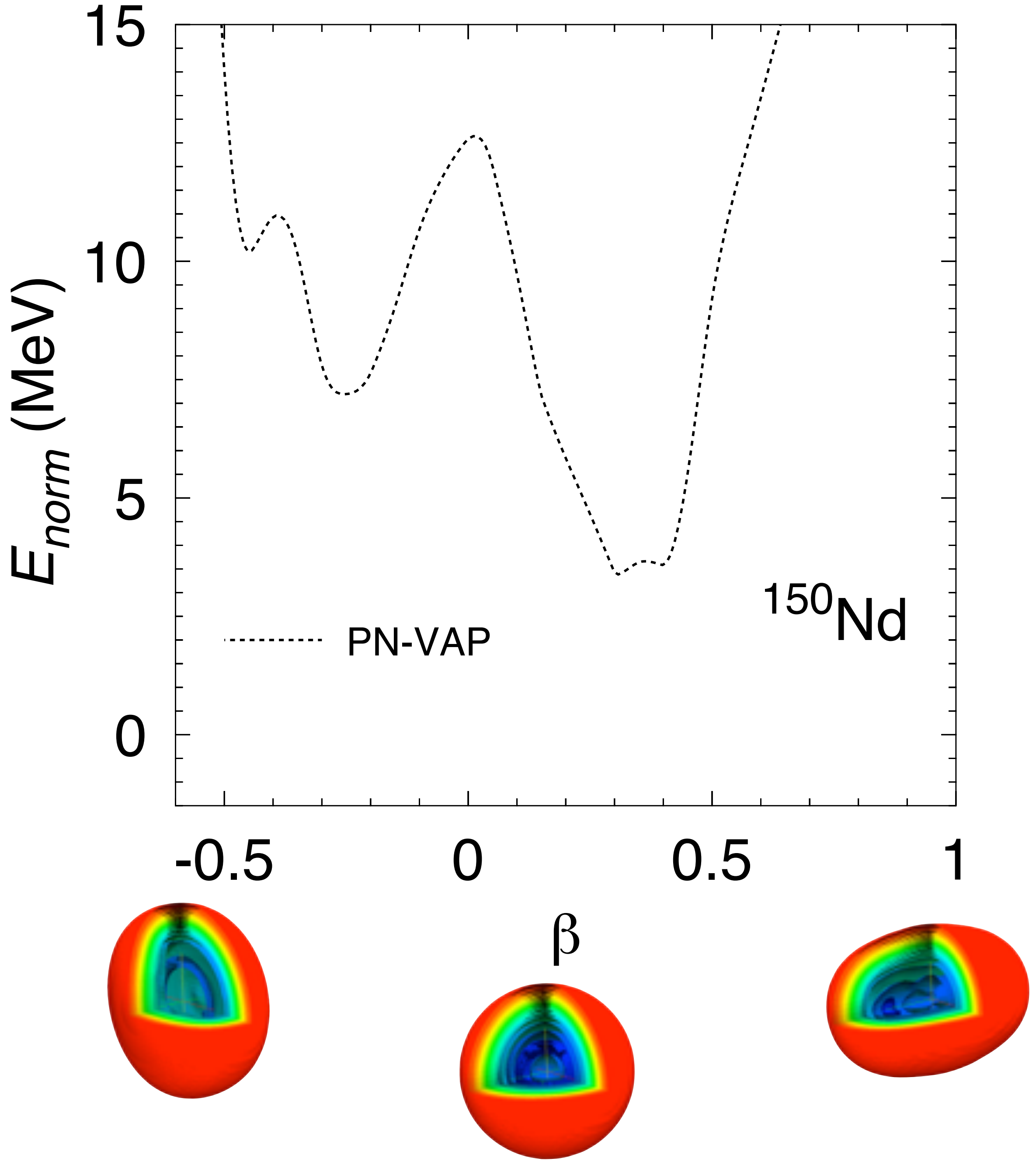

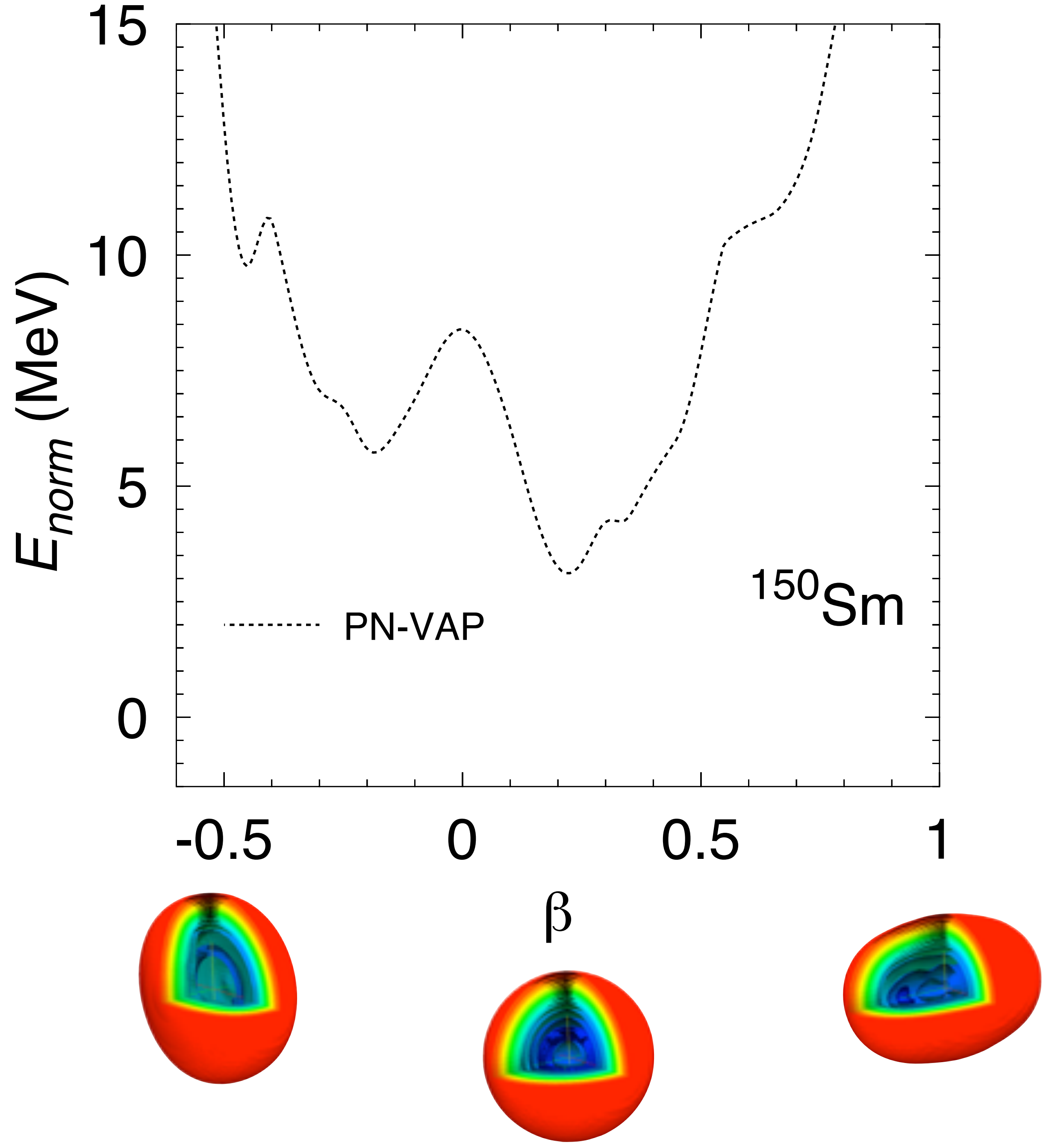

Determination of initial and final states (II)

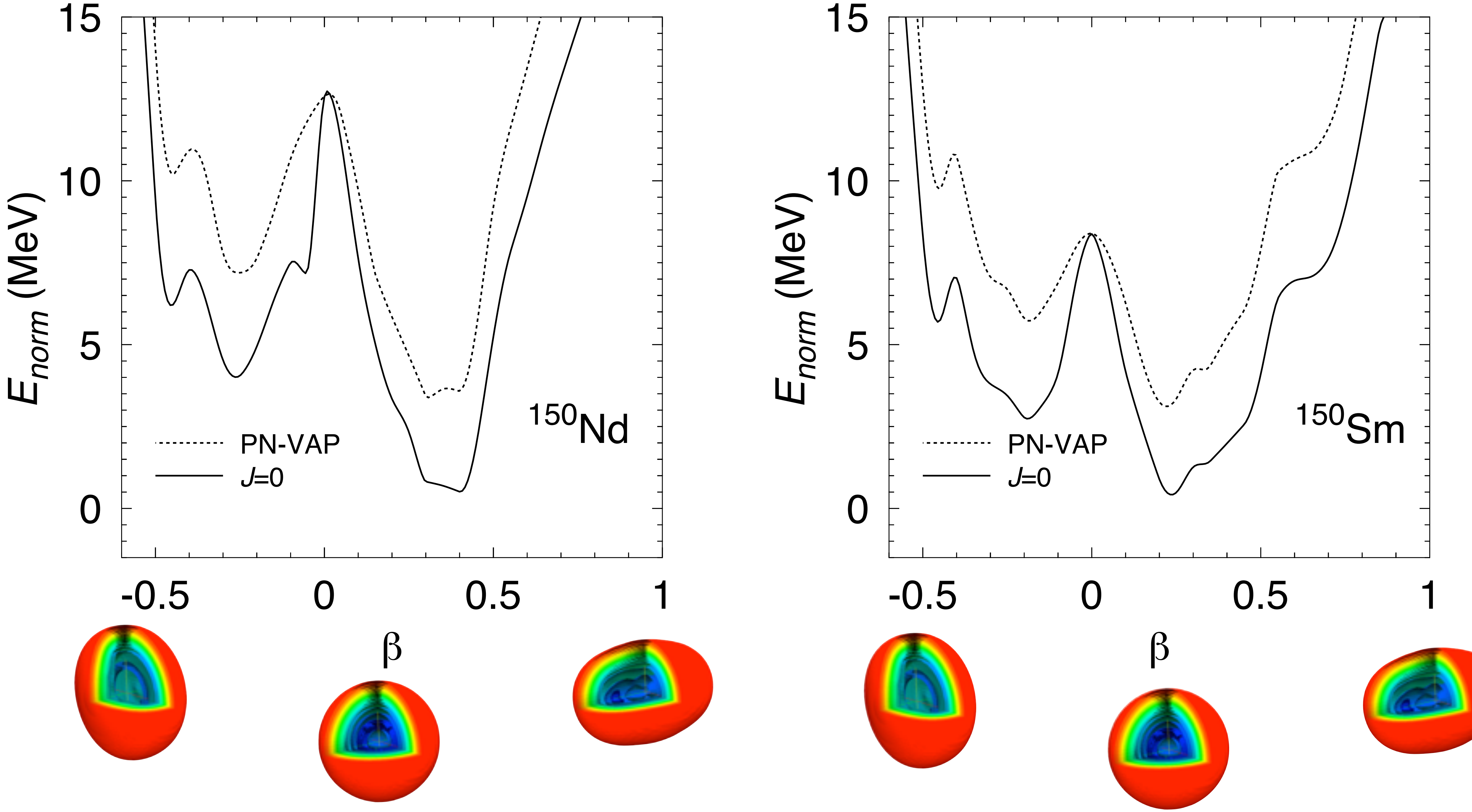

EDF axial

Determination of initial and final states (and III)

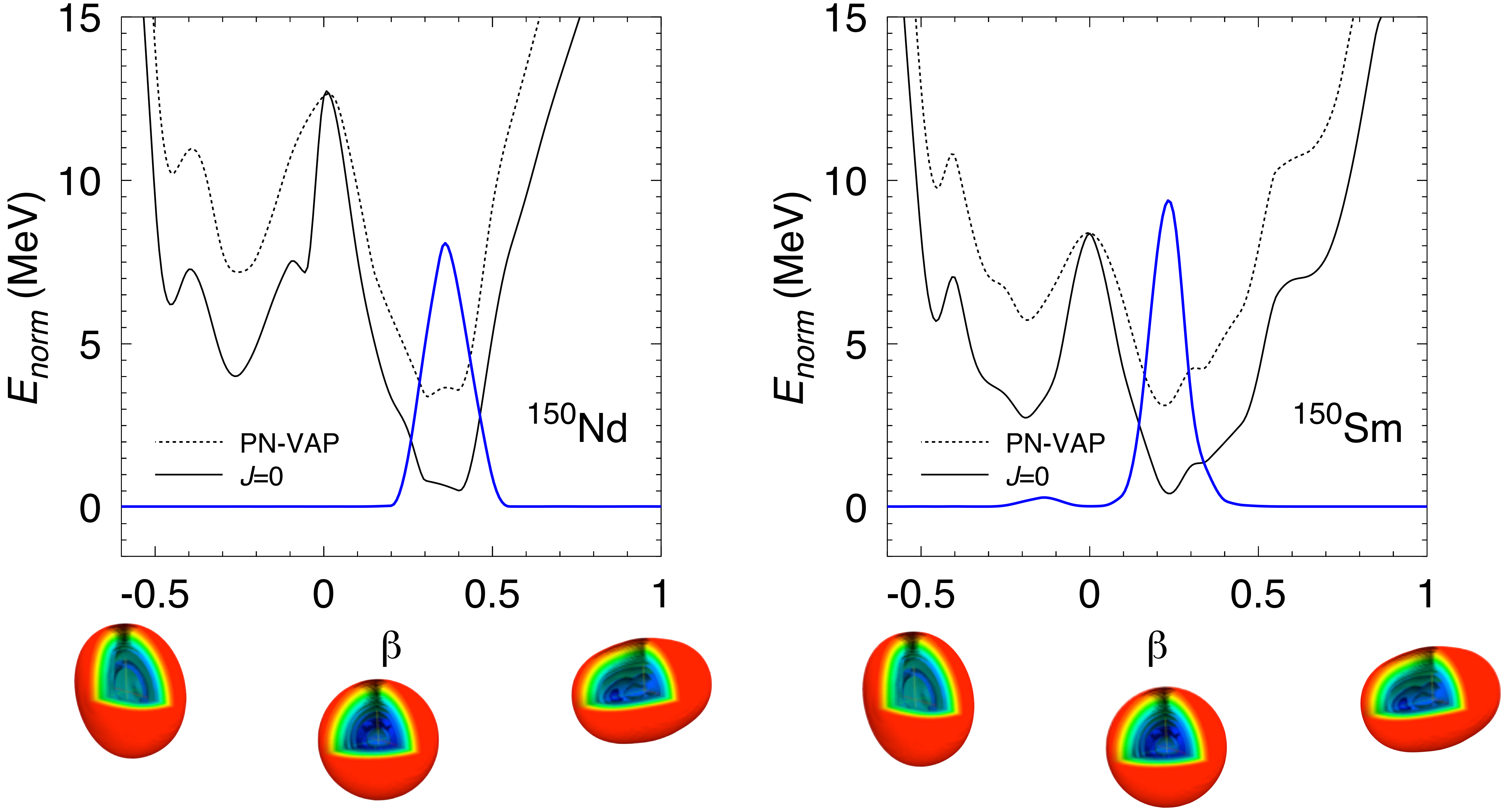

EDF axial

1. Axial states $K=0$
2. Angular momentum $I=0$
3. Quadrupole deformations $q=q_{20}$
4. Quadrupole and pairing pp/nn correlations $q=(q_{20},\delta)$
5. Quadrupole and pn correlations $q=(q_{20},p_0)$
6. Quadrupole and octupole deformations $q=(q_{20},q_{30})$

$\longrightarrow$

$$|0;N_iZ_i;\sigma\rangle = \sum_{\Lambda_i} G_{\Lambda_i}^{0;N_iZ_i;\sigma}|\Lambda_i^{0;N_iZ_i}\rangle$$

$$|0;N_fZ_f;\sigma\rangle = \sum_{\Lambda_f} G_{\Lambda_f}^{0;N_fZ_f;\sigma}|\Lambda_f^{0;N_fZ_f}\rangle$$

EDF axial

1. Axial states $K=0$
2. Angular momentum $I=0$
3. Quadrupole deformations $q=q_{20}$
4. Quadrupole and pairing pp/nn correlations $q=(q_{20},\delta)$
5. Quadrupole and pn correlations $q=(q_{20},p_0)$
6. Quadrupole and octupole deformations $q=(q_{20},q_{30})$

$\longrightarrow$

$$|0;N_iZ_i;\sigma\rangle = \sum_{\Lambda_i} G^{0;N_iZ_i;\sigma}_{\Lambda_i}|\Lambda^{0;N_iZ_i}_i\rangle$$

$$|0;N_fZ_f;\sigma\rangle = \sum_{\Lambda_f} G^{0;N_fZ_f;\sigma}_{\Lambda_f}|\Lambda^{0;N_fZ_f}_f\rangle$$

TRANSITIONS:

$$M^{0\nu\beta\beta}_{\xi} = \langle 0^+_f|\hat{O}^{0\nu\beta\beta}_{\xi}|0^+_i\rangle = \langle 0;N_fZ_f|\hat{O}^{0\nu\beta\beta}_{\xi}|0;N_iZ_i\rangle =$$

$$\sum_{\Lambda_f\Lambda_i}\left(G^{0;N_fZ_f}_{\Lambda_f}\right)^*\langle\Lambda^{0;N_fZ_f}_f|\hat{O}^{0\nu\beta\beta}_{\xi}|\Lambda^{0;N_iZ_i}_i\rangle G^{0;N_iZ_i}_{\Lambda_i} = \sum_{q_iq_f;\Lambda_f\Lambda_i}$$

$$\left(\frac{u^{0;N_fZ_f}_{q_f,\Lambda_f}}{\sqrt{n^{0;N_fZ_f}_{\Lambda_f}}}\right)^*\left(G^{0;N_fZ_f}_{\Lambda_f}\right)^*\langle 0;N_fZ_f;q_f|\hat{O}^{0\nu\beta\beta}_{\xi}|0;N_iZ_i;q_i\rangle\left(G^{0;N_iZ_i}_{\Lambda_i}\right)\left(\frac{u^{0;N_iZ_i}_{q_i,\Lambda_i}}{\sqrt{n^{0;N_iZ_i}_{\Lambda_i}}}\right)$$

EDF axial

UAM UNIVERSIDAD AUTONOMA DE MADRID

1. Axial states $K = 0$
2. Angular momentum $I = 0$
3. Quadrupole deformations $q = q_{20}$
4. Quadrupole and pairing pp/nn correlations $q = (q_{20}, \delta)$
5. Quadrupole and pn correlations $q = (q_{20}, p_0)$
6. Quadrupole and octupole deformations $q = (q_{20}, q_{30})$

$\longrightarrow$

$$|0; N_iZ_i;\sigma\rangle = \sum_{\Lambda_i} G^{0;N_iZ_i;\sigma}_{\Lambda_i}|\Lambda^{0;N_iZ_i}_i\rangle$$

$$|0; N_fZ_f;\sigma\rangle = \sum_{\Lambda_f} G^{0;N_fZ_f;\sigma}_{\Lambda_f}|\Lambda^{0;N_fZ_f}_f\rangle$$

TRANSITIONS:

$$M^{0\nu\beta\beta}_{\xi} = \langle 0^+_f|\hat{O}^{0\nu\beta\beta}_{\xi}|0^+_i\rangle = \langle 0; N_fZ_f|\hat{O}^{0\nu\beta\beta}_{\xi}|0; N_iZ_i\rangle =$$

$$\sum_{\Lambda_f\Lambda_i}\left(G^{0;N_fZ_f}_{\Lambda_f}\right)^*\langle\Lambda^{0;N_fZ_f}_f|\hat{O}^{0\nu\beta\beta}_{\xi}|\Lambda^{0;N_iZ_i}_i\rangle G^{0;N_iZ_i}_{\Lambda_i} = \sum_{q_iq_f;\Lambda_f\Lambda_i}$$

$$\left(\frac{u^{0;N_fZ_f}_{q_f,\Lambda_f}}{\sqrt{n^{0;N_fZ_f}_{\Lambda_f}}}\right)^*\left(G^{0;N_fZ_f}_{\Lambda_f}\right)^*\langle 0; N_fZ_f;q_f|\hat{O}^{0\nu\beta\beta}_{\xi}|0; N_iZ_i;q_i\rangle\left(G^{0;N_iZ_i}_{\Lambda_i}\right)\left(\frac{u^{0;N_iZ_i}_{q_i,\Lambda_i}}{\sqrt{n^{0;N_iZ_i}_{\Lambda_i}}}\right)$$

Matrix elements of the double beta transition operators between particle number and angular momentum projected states

NME: axial quadrupole deformation

UNIVERSIDAD AUTONOMA DE MADRID

$$\frac{\langle 0; N_f Z_f; q_f | \hat{O}^{0\nu\beta\beta}_{\xi} | 0; N_i Z_i; q_i \rangle}{\sqrt{\langle 0; N_f Z_f; q_f | 0; N_f Z_f; q_f \rangle \langle 0; N_i Z_i; q_i | 0; N_i Z_i; q_i \rangle}}$$

A=150

T.R.R., Martínez-Pinedo, PRL 105, 252503 (2010)

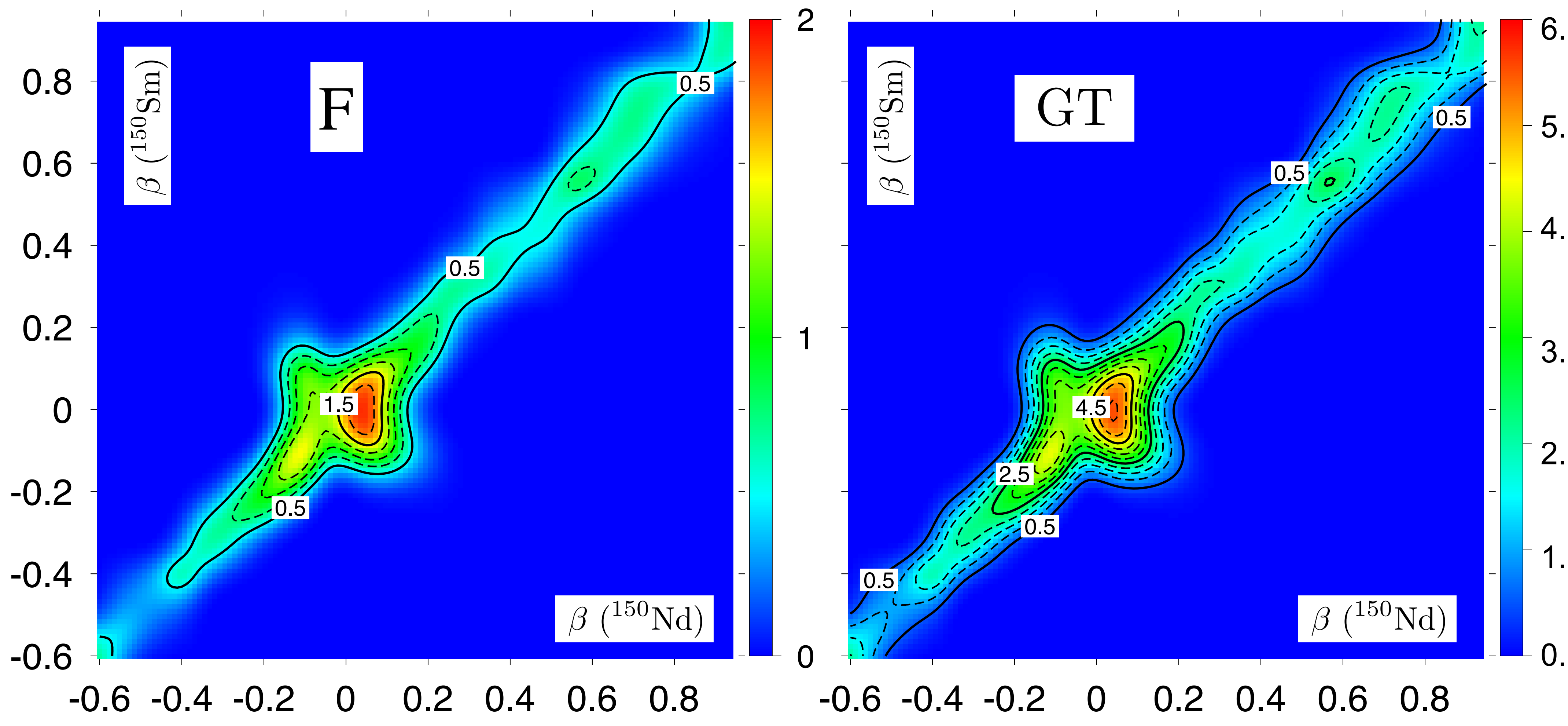

- GT strength greater than Fermi.
- Similar deformation between mother and granddaughter is favored by the transition operators
- Maxima are found close to sphericity although some other local maxima are found

NME: axial quadrupole deformation

$$\frac{\langle 0;N_fZ_f;q_f|\hat{O}^{0\nu\beta\beta}_{\xi}|0;N_iZ_i;q_i\rangle}{\sqrt{\langle 0;N_fZ_f;q_f|0;N_fZ_f;q_f\rangle\langle 0;N_iZ_i;q_i|0;N_iZ_i;q_i\rangle}}$$

A=150

T.R.R., Martínez-Pinedo, PRL 105, 252503 (2010)

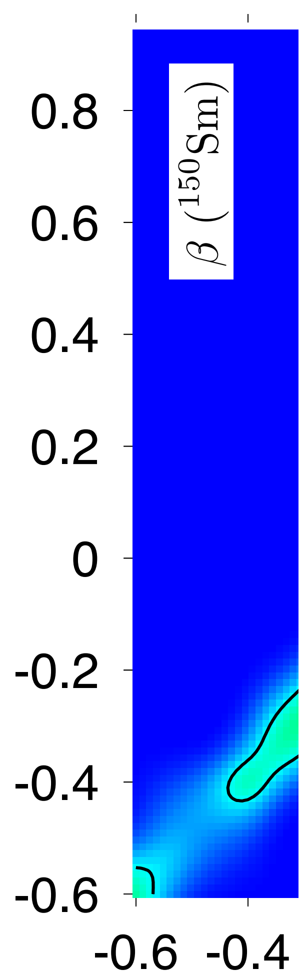

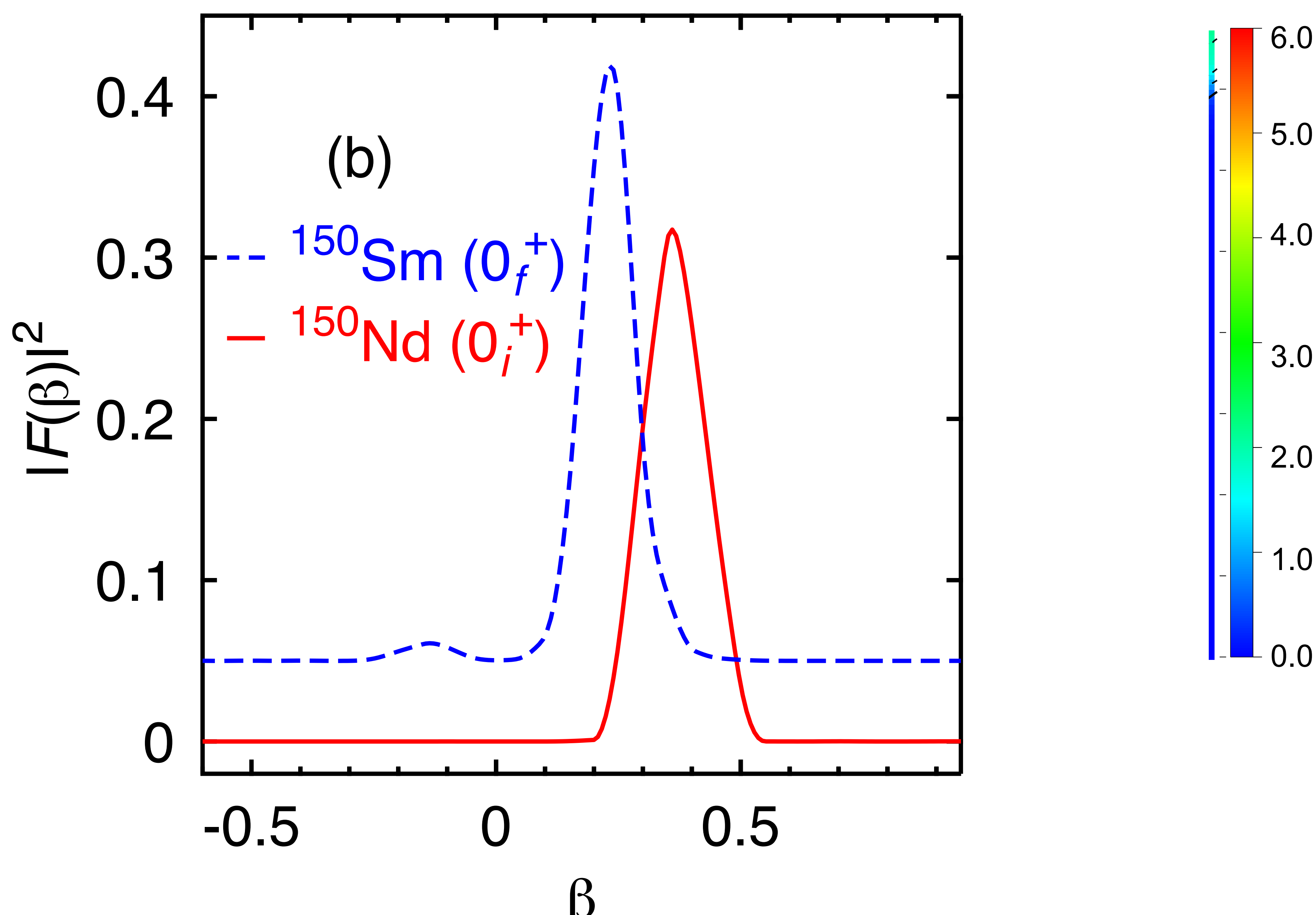

- GT streng
- Similar de
- Maxima a

- Final result depends on the distribution of probability of the corresponding initial and final collective states within this plot

NME: axial quadrupole deformation

$$\frac{\langle 0; N_f Z_f; q_f | \hat{O}_{\xi}^{0\nu\beta\beta} | 0; N_i Z_i; q_i \rangle}{\sqrt{\langle 0; N_f Z_f; q_f | 0; N_f Z_f; q_f \rangle \langle 0; N_i Z_i; q_i | 0; N_i Z_i; q_i \rangle}}$$

A=150

T.R.R., Martínez-Pinedo, PRL 105, 252503 (2010)

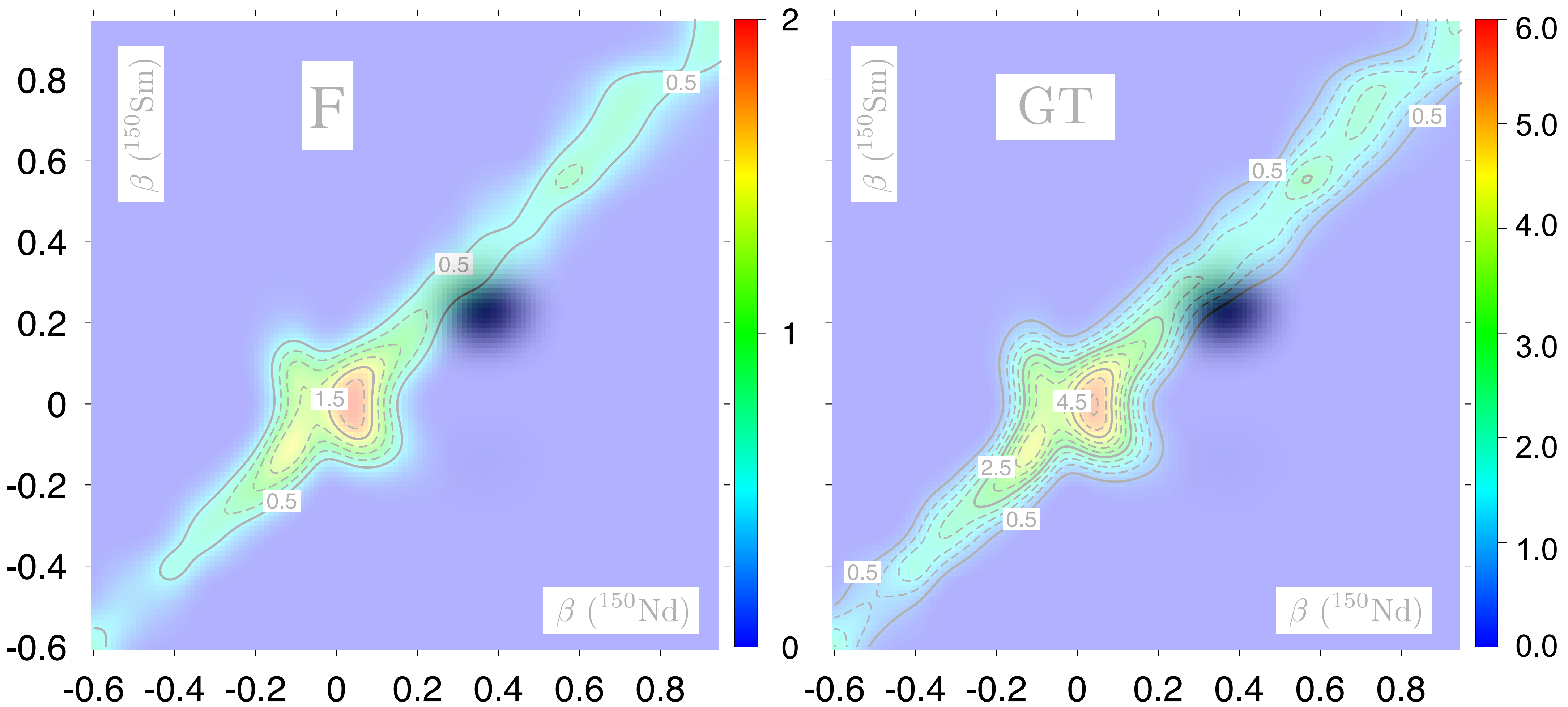

- GT strength greater than Fermi.
- Similar deformation between mother and granddaughter is favored by the transition operators
- Maxima are found close to sphericity although some other local maxima are found
- Final result depends on the distribution of probability of the corresponding initial and final collective states within this plot

NME: axial quadrupole deformation

$$\frac{\langle 0;N_fZ_f;q_f|\hat{O}^{0\nu\beta\beta}_{\xi}|0;N_iZ_i;q_i\rangle}{\sqrt{\langle 0;N_fZ_f;q_f|0;N_fZ_f;q_f\rangle\langle 0;N_iZ_i;q_i|0;N_iZ_i;q_i\rangle}}$$

A=150

T.R.R., Martínez-Pinedo, PRL 105, 252503 (2010)

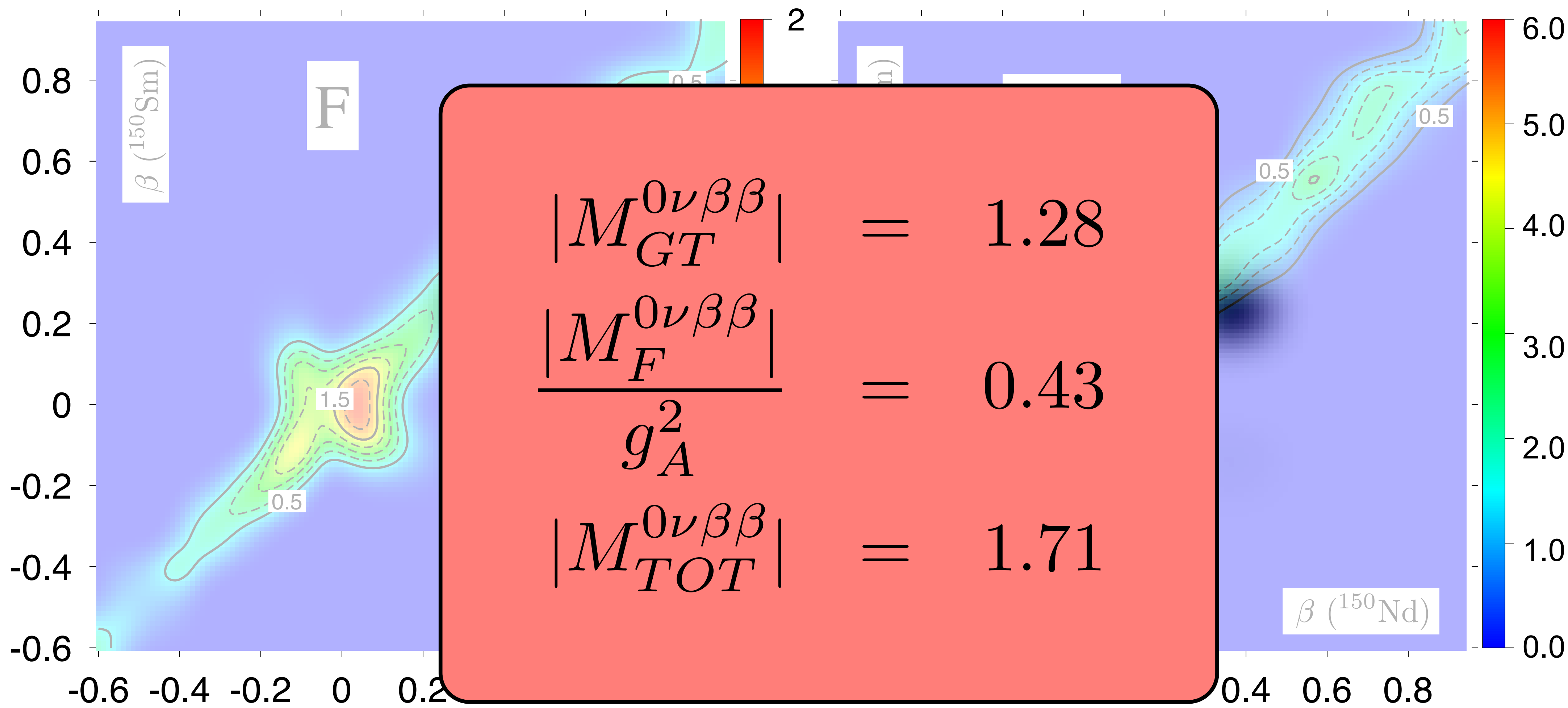

$$|M^{0\nu\beta\beta}_{GT}| = 1.28$$

$$\frac{|M^{0\nu\beta\beta}_{F}|}{g_A^2} = 0.43$$

$$|M^{0\nu\beta\beta}_{TOT}| = 1.71$$

- GT strength greater than Fermi.
- Similar deformation between mother and granddaughter is favored by the transition operators
- Maxima are found close to sphericity although some other local maxima are found
- Final result depends on the distribution of probability of the corresponding initial and final collective states within this plot

NME: axial quadrupole plus octupole deformation

J. M. Yao and J. Engel, arXiv 1604.06297 (2016)

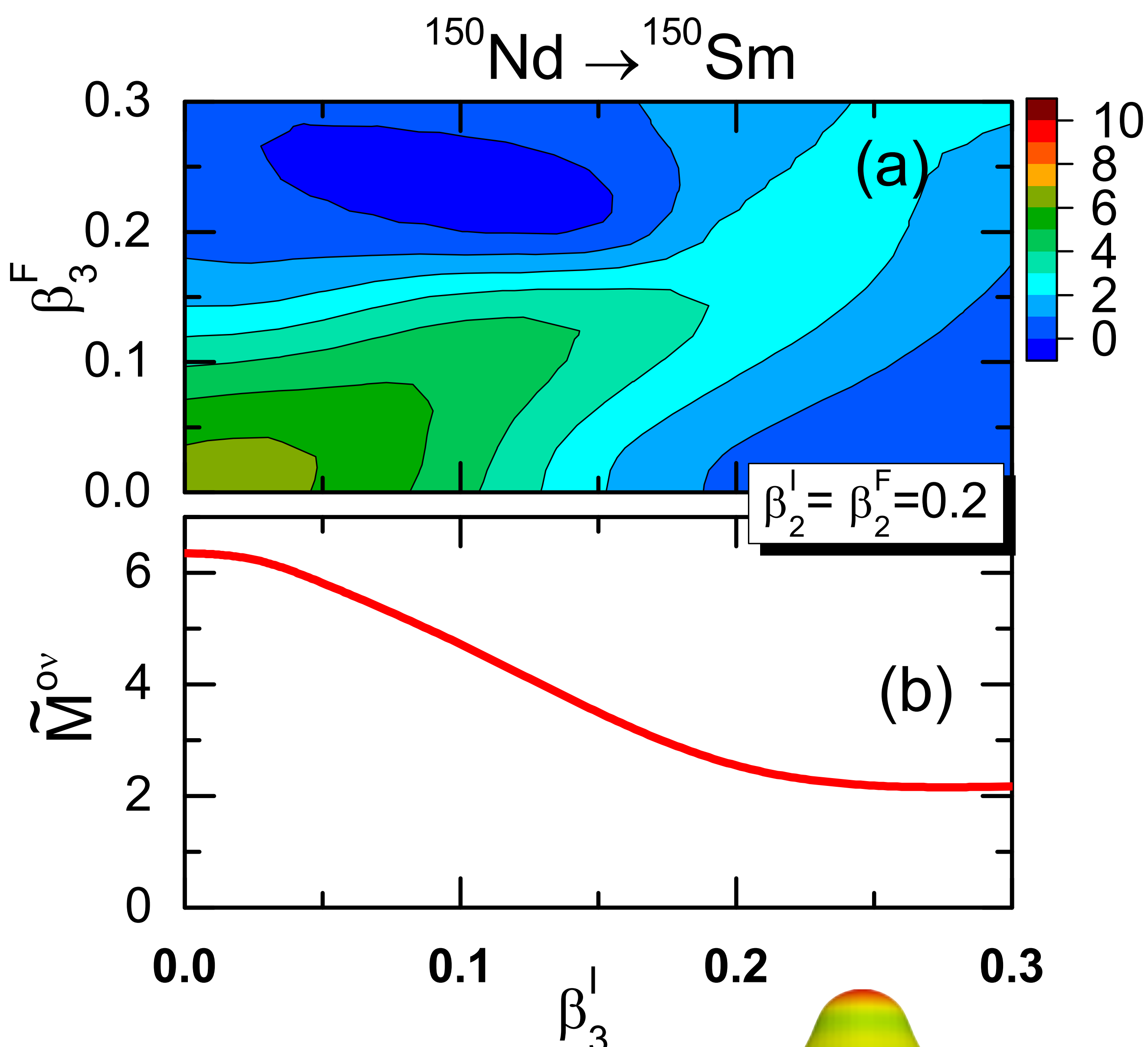

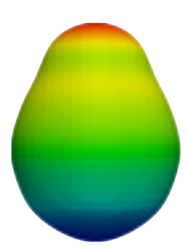

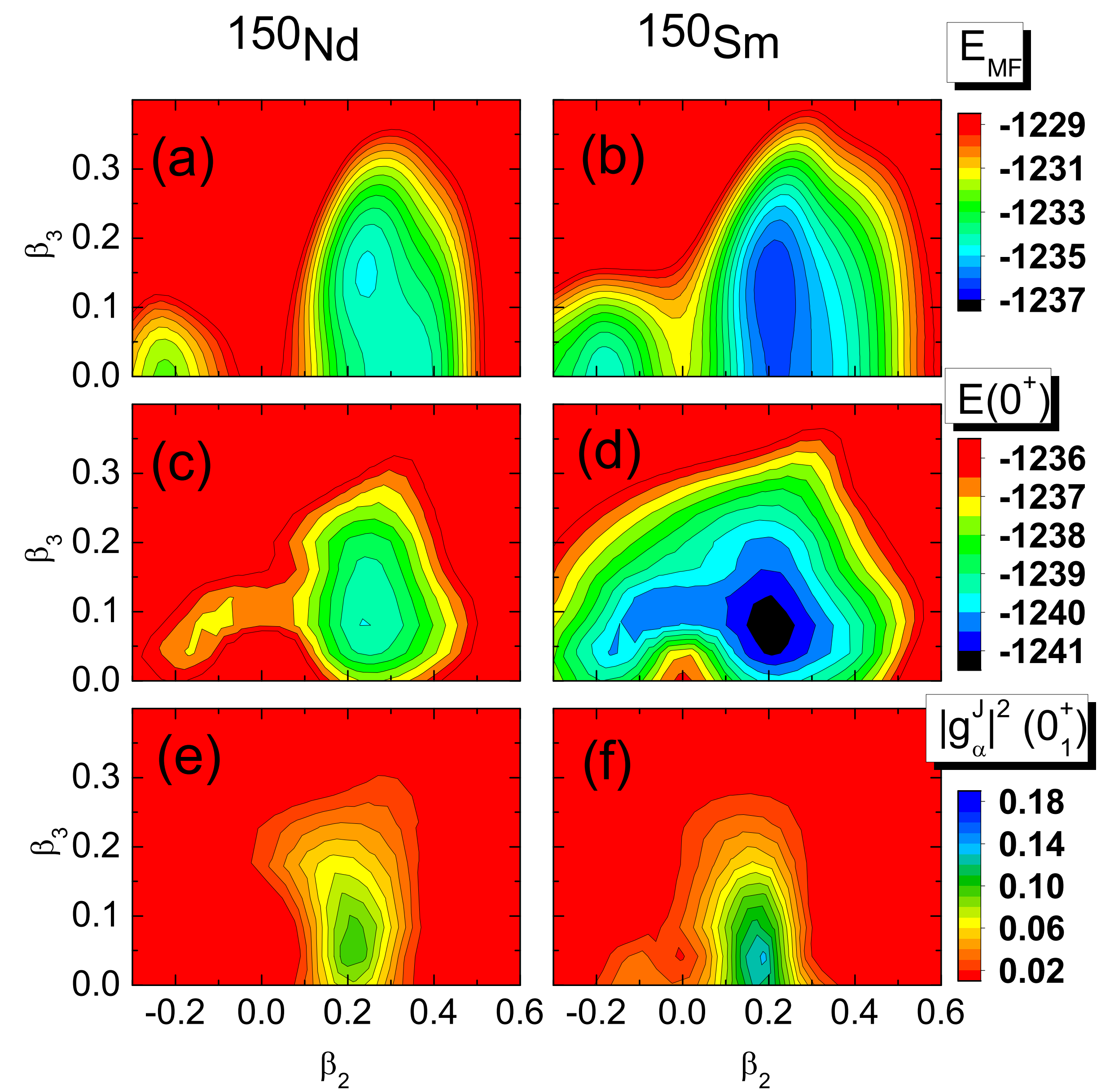

NME: axial quadrupole plus octupole deformation

J. M. Yao and J. Engel, arXiv 1604.06297 (2016)

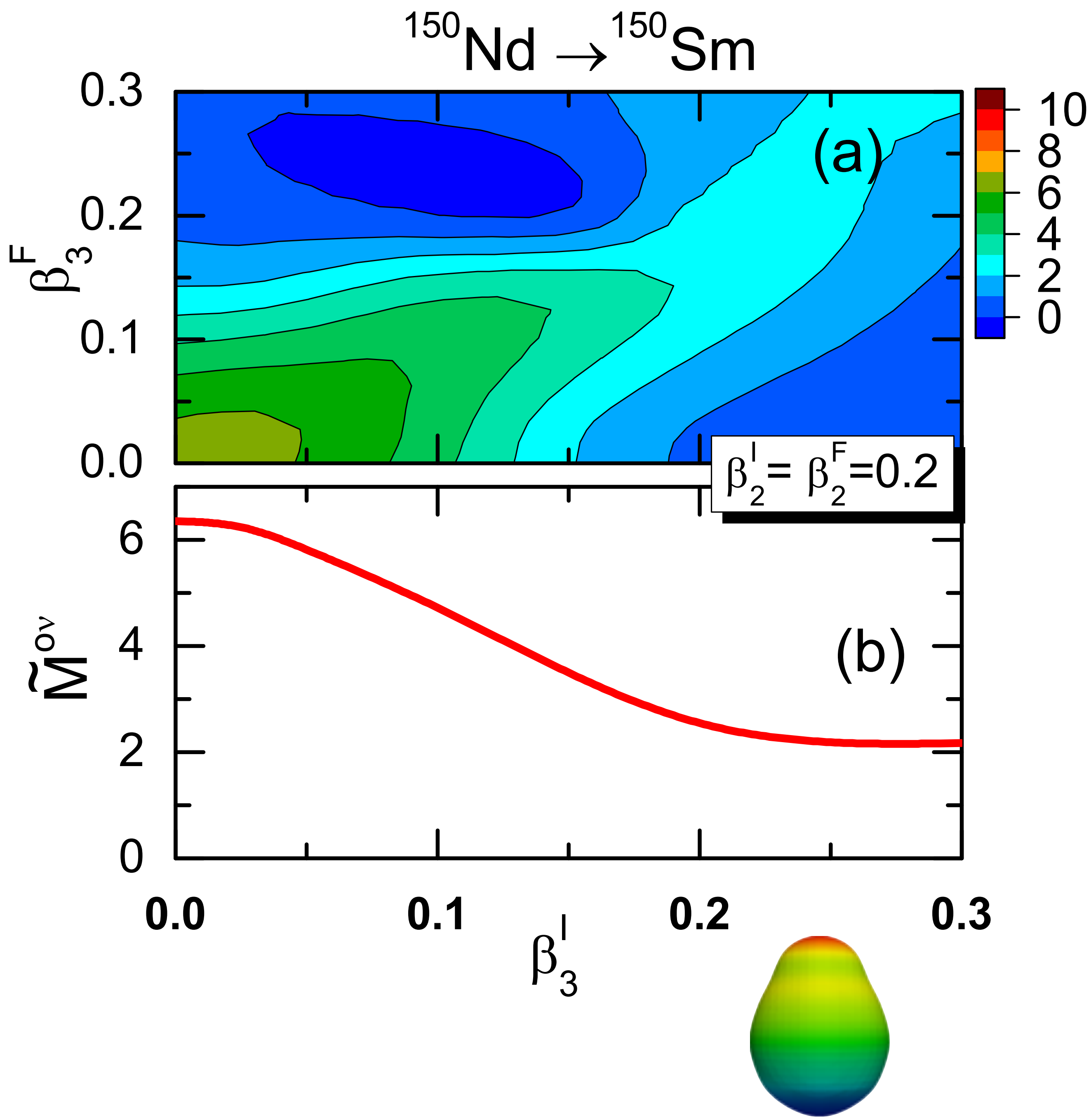

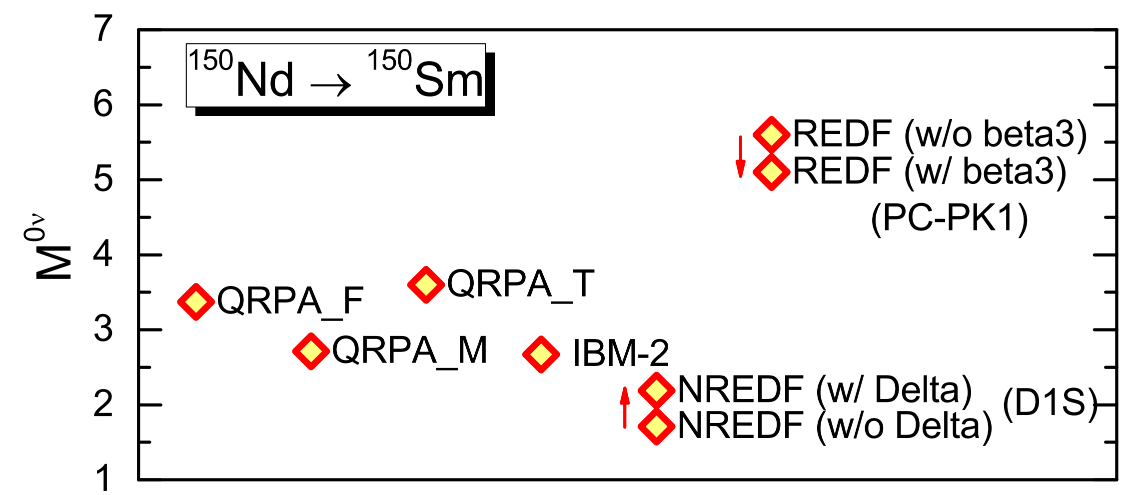

FIG. 5: (Color online) The final matrix element $M^{0\nu}$ from the GCM calculation with and without [46] octupole shape fluctuations (REDF) and those of the QRPA ("QRPA_F" [66], "QRPA_M" [45], "QRPA_T" [47]), the IMB-2 [67], and the non-relativistic GCM, based on the Gogny D1S interaction, with [68] and without [44] pairing fluctuations.

A=76

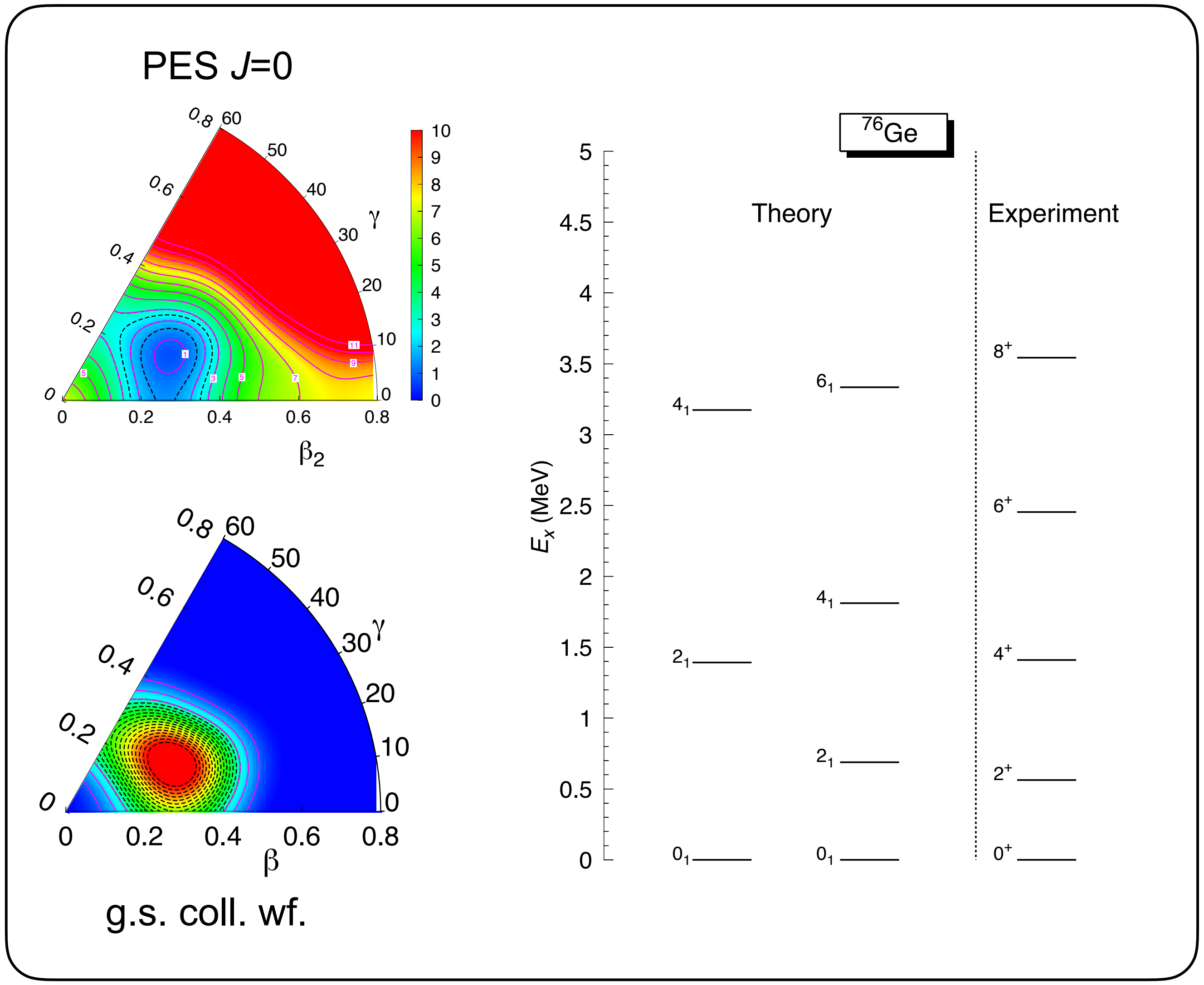

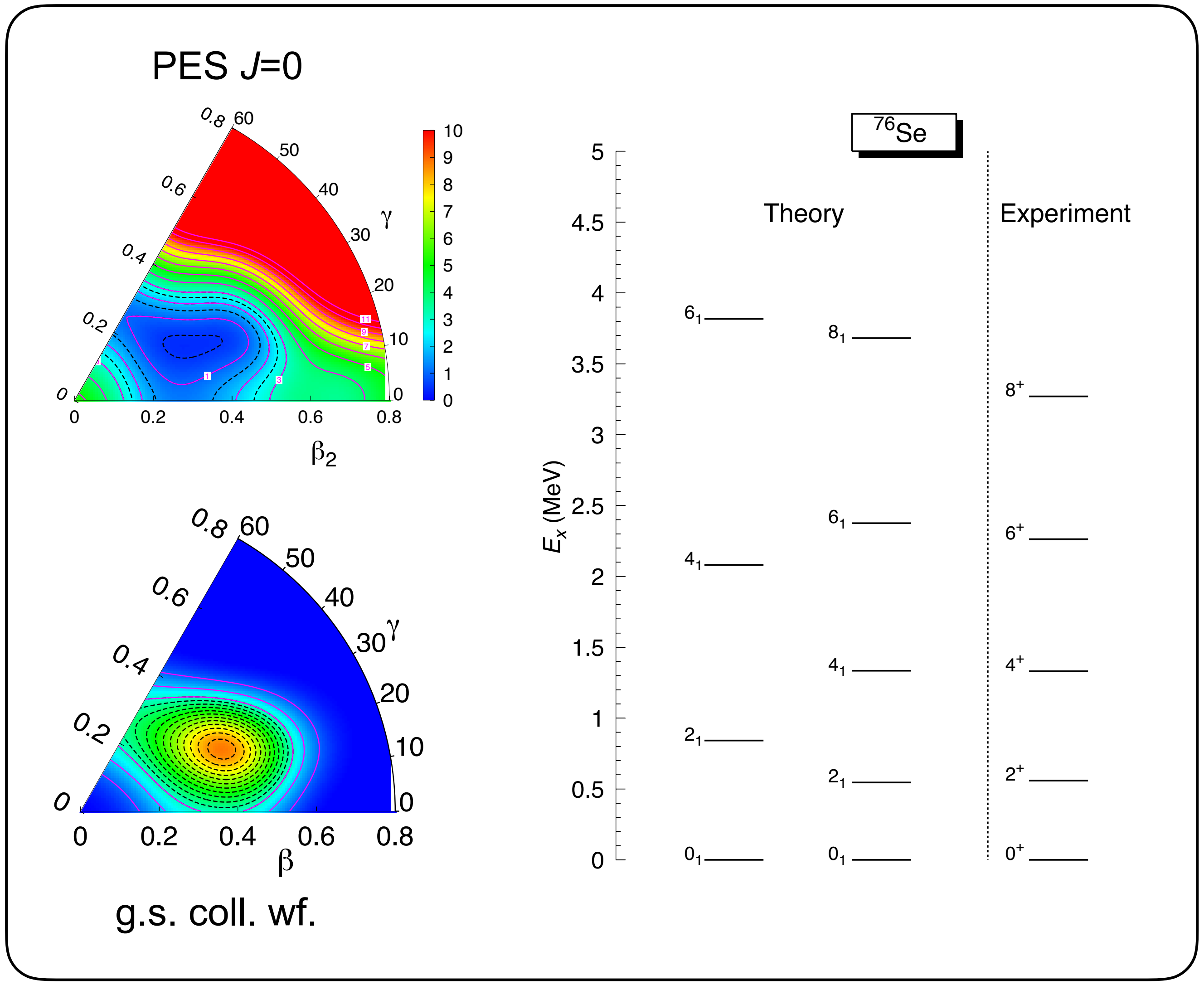

T.R.R., in progress

A=76

PES *J*=0

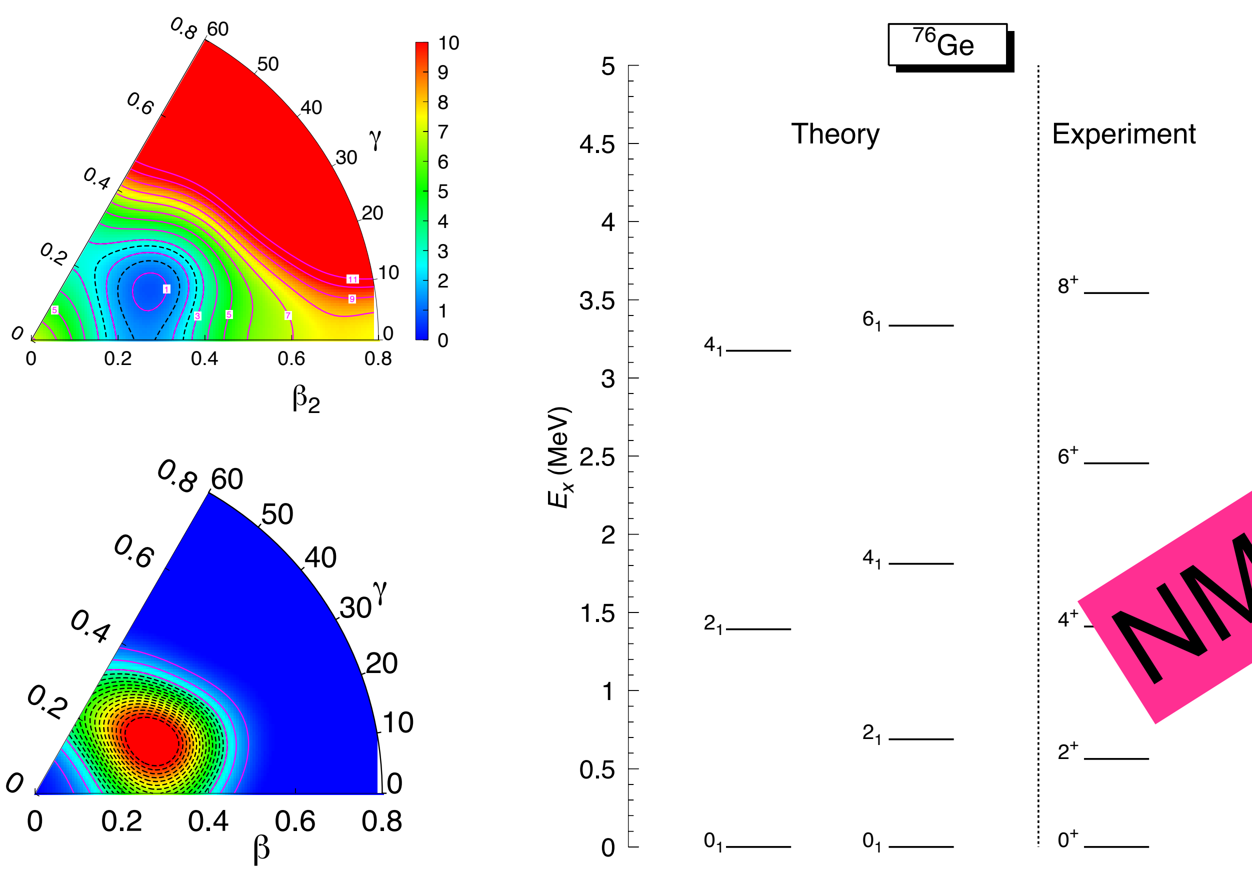

g.s. coll. wf.

NME??

PES *J*=0

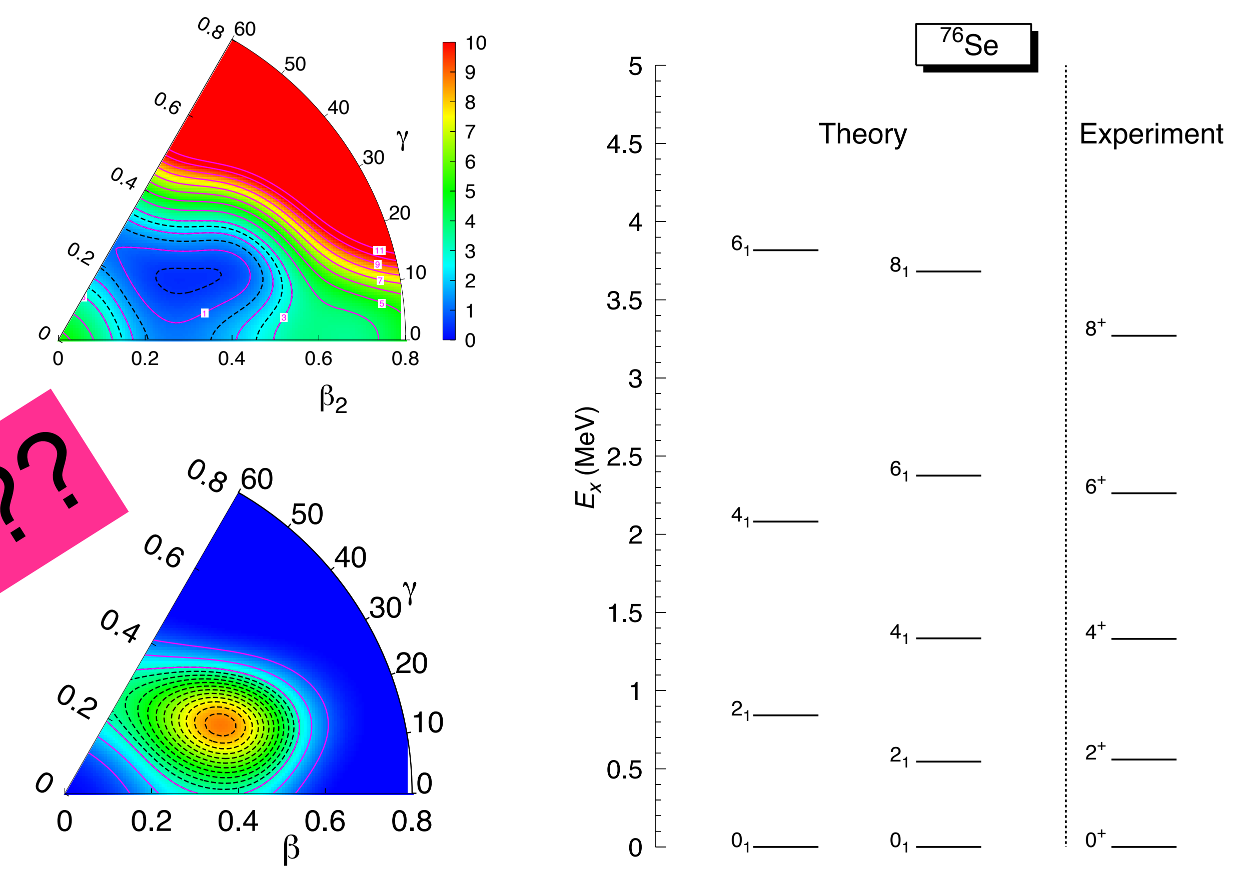

g.s. coll. wf.

T.R.R., in progress

NME: triaxial quadrupole deformation

UNIVERSIDAD AUTONOMA DE MADRID

HFB-PES

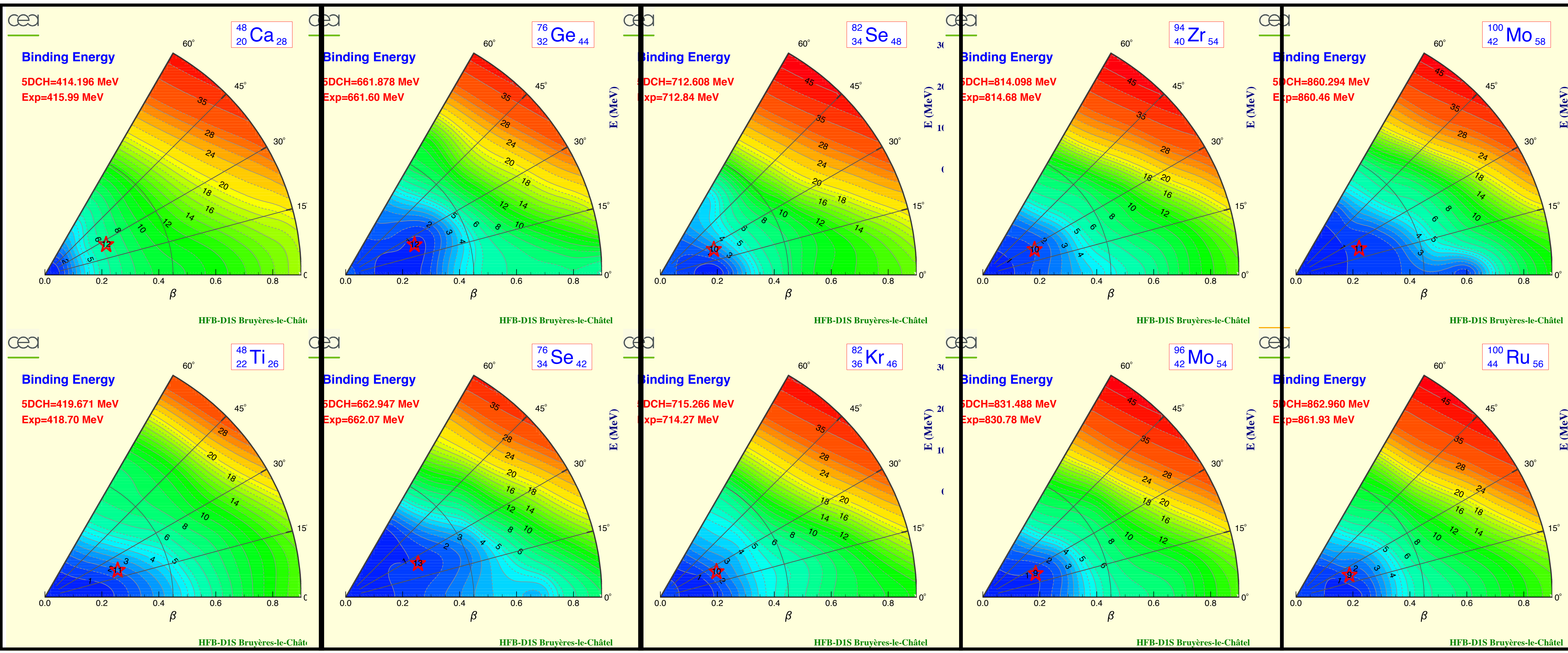

CEA-Bruyeres-le-Chatel data base

NME: triaxial quadrupole deformation

HFB-PES

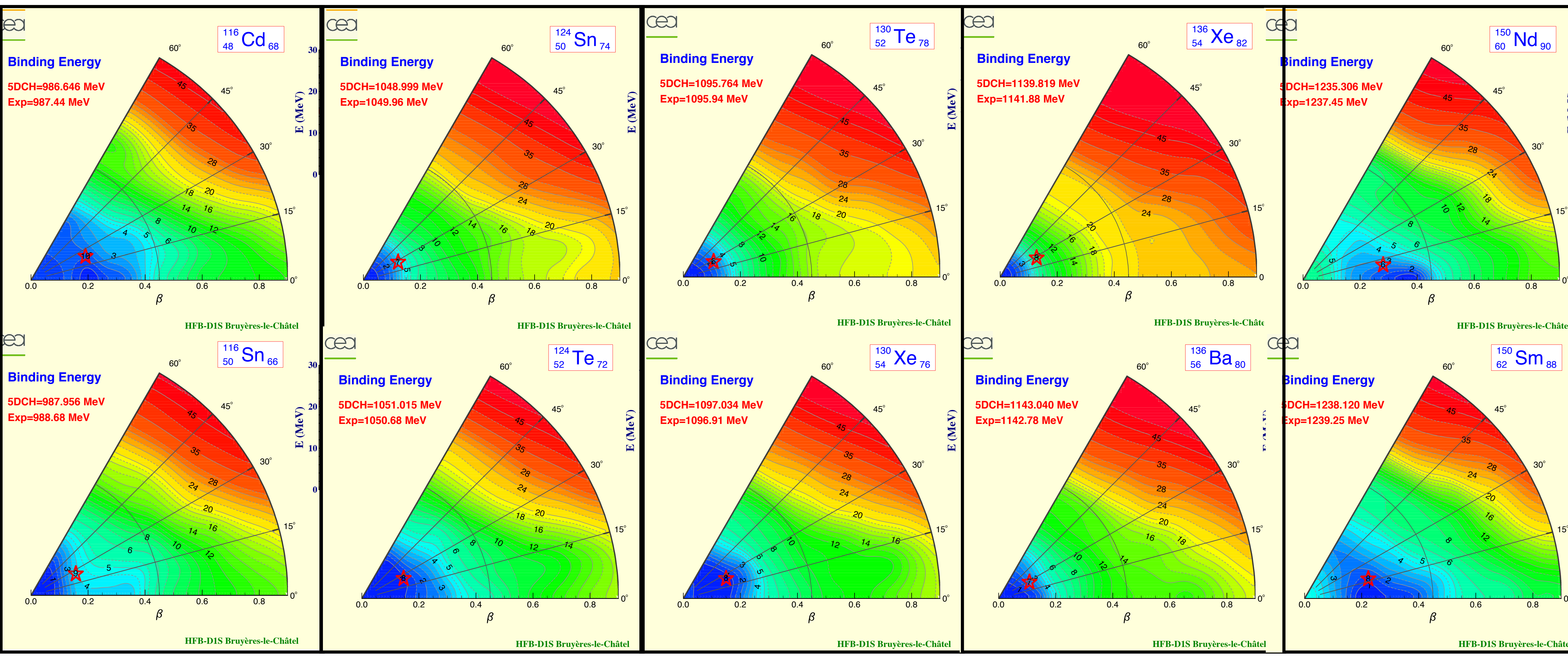

CEA-Bruyeres-le-Chatel data base

NME: Shape and pp/nn pairing fluctuations

Angular momentum projected potential energy surfaces

Collective ground state wave functions

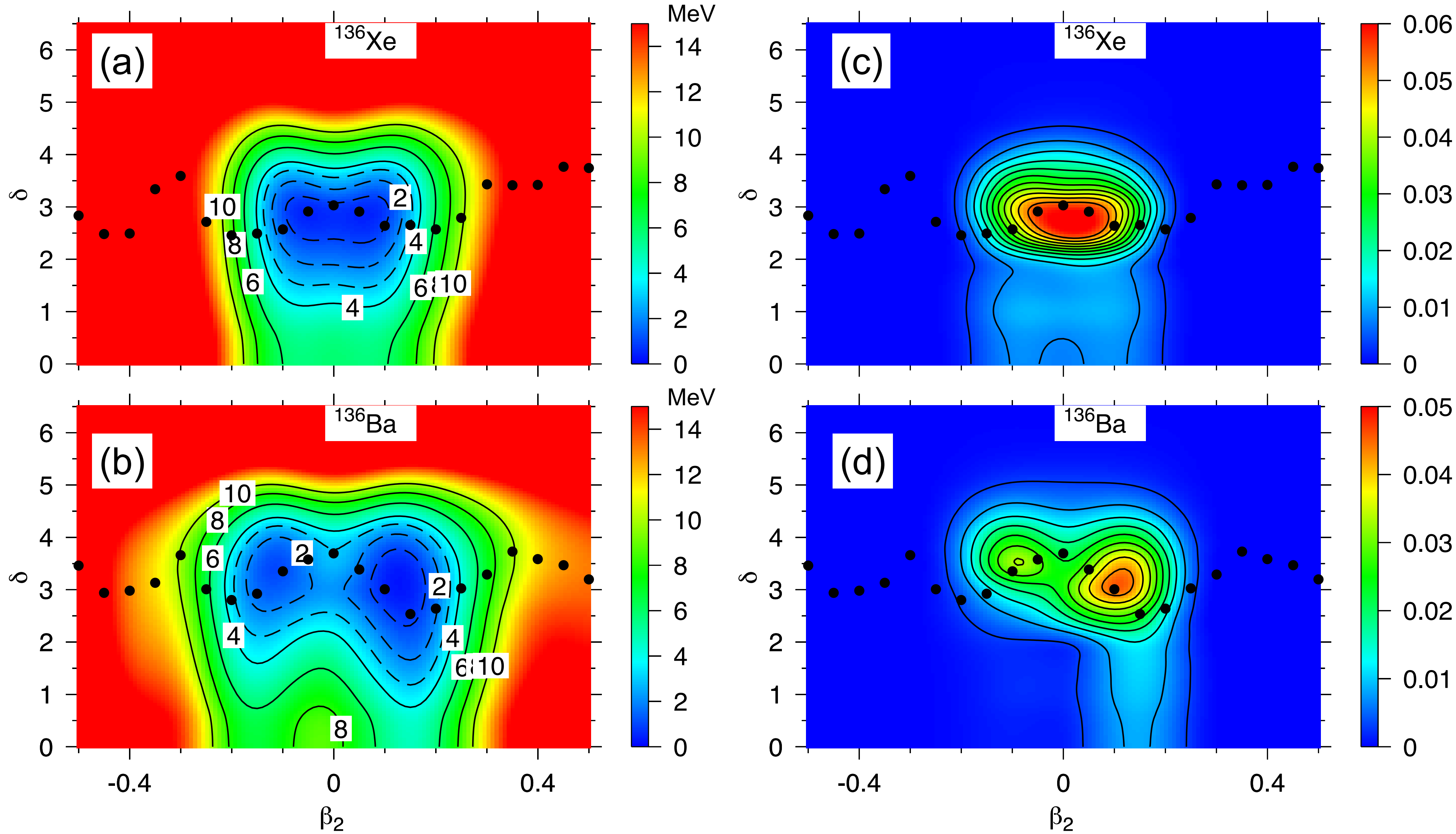

N. López-Vaquero, T.R.R., J.L. Egido, PRL 111, 142501 (2013)

NME: Shape and pp/nn pairing fluctuations

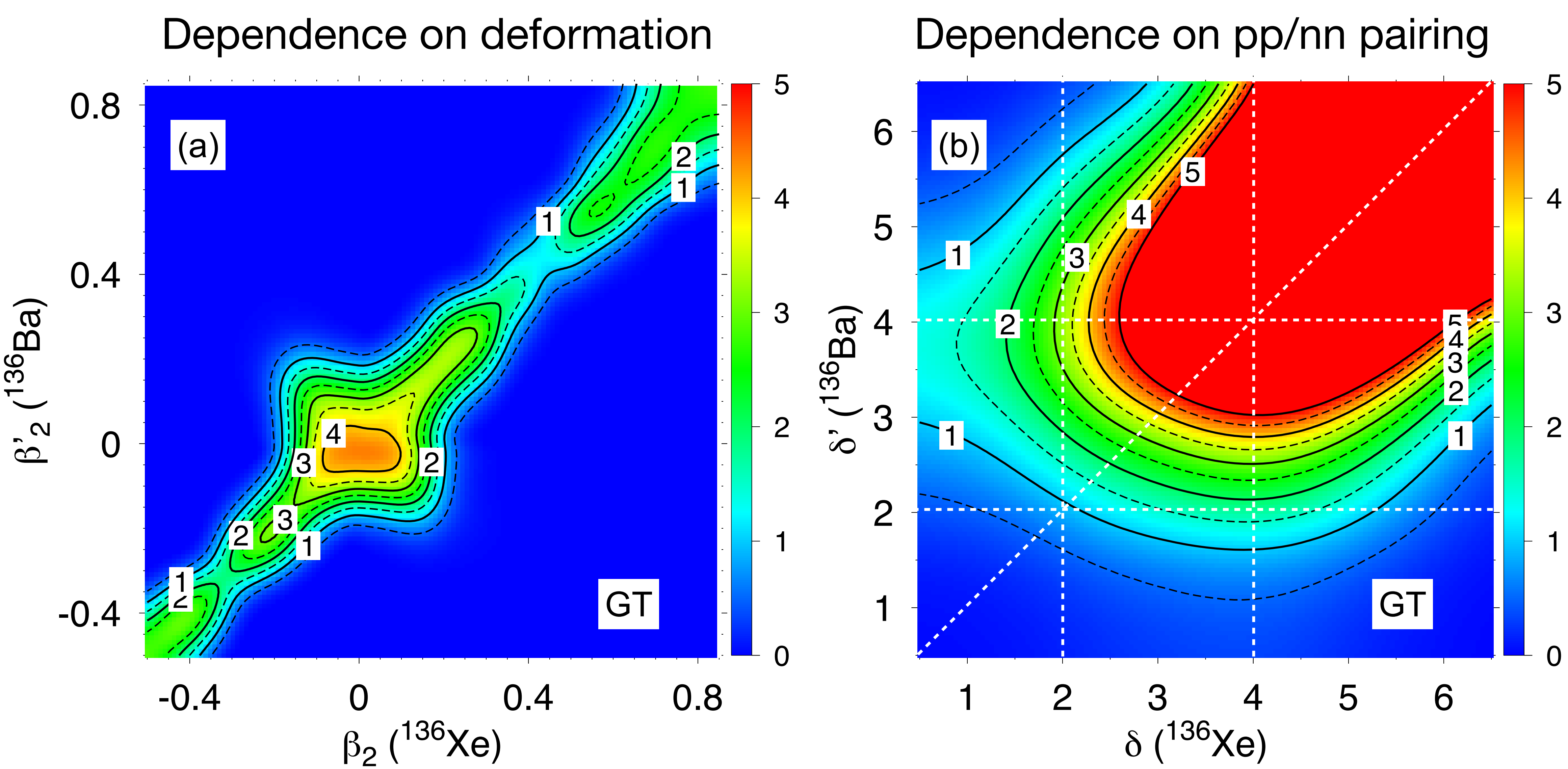

N. López-Vaquero, T.R.R., J.L. Egido, PRL 111, 142501 (2013)

NME: Shape and pn pairing fluctuations

$$H = h_0 - \sum_{\mu=-1}^{1} g_{\mu}^{T=1}\, S_{\mu}^{\dagger} S_{\mu} - \frac{\chi}{2} \sum_{K=-2}^{2} Q_{2K}^{\dagger} Q_{2K}$$
$$- g^{T=0} \sum_{\nu=-1}^{1} P_{\nu}^{\dagger} P_{\nu} + g_{ph} \sum_{\mu,\nu=-1}^{1} F_{\nu}^{\mu\dagger} F_{\nu}^{\mu}\,, \qquad (2)$$

where h_0 contains spherical single particle energies, Q_{2K} are the components of a quadrupole operator defined in Ref. [15], and

$$S_{\mu}^{\dagger} = \frac{1}{\sqrt{2}} \sum_{l} \hat{l} [c_l^{\dagger} c_l^{\dagger}]^{001}_{00\mu}\,, \quad P_{\mu}^{\dagger} = \frac{1}{\sqrt{2}} \sum_{l} \hat{l} [c_l^{\dagger} c_l^{\dagger}]^{010}_{0\mu 0}\,,$$
$$F_{\nu}^{\mu} = \frac{1}{2} \sum_{i} \sigma_i^{\mu} \tau_i^{\nu} = \sum_{l} \hat{l} [c_l^{\dagger} \bar{c}_l]^{011}_{0\mu\nu}\,. \qquad (3)$$

$$H' = H - \lambda_Z N_Z - \lambda_N N_N - \lambda_Q Q_{20} - \frac{\lambda_P}{2}\left(P_0 + P_0^{\dagger}\right)\,, \quad (6)$$

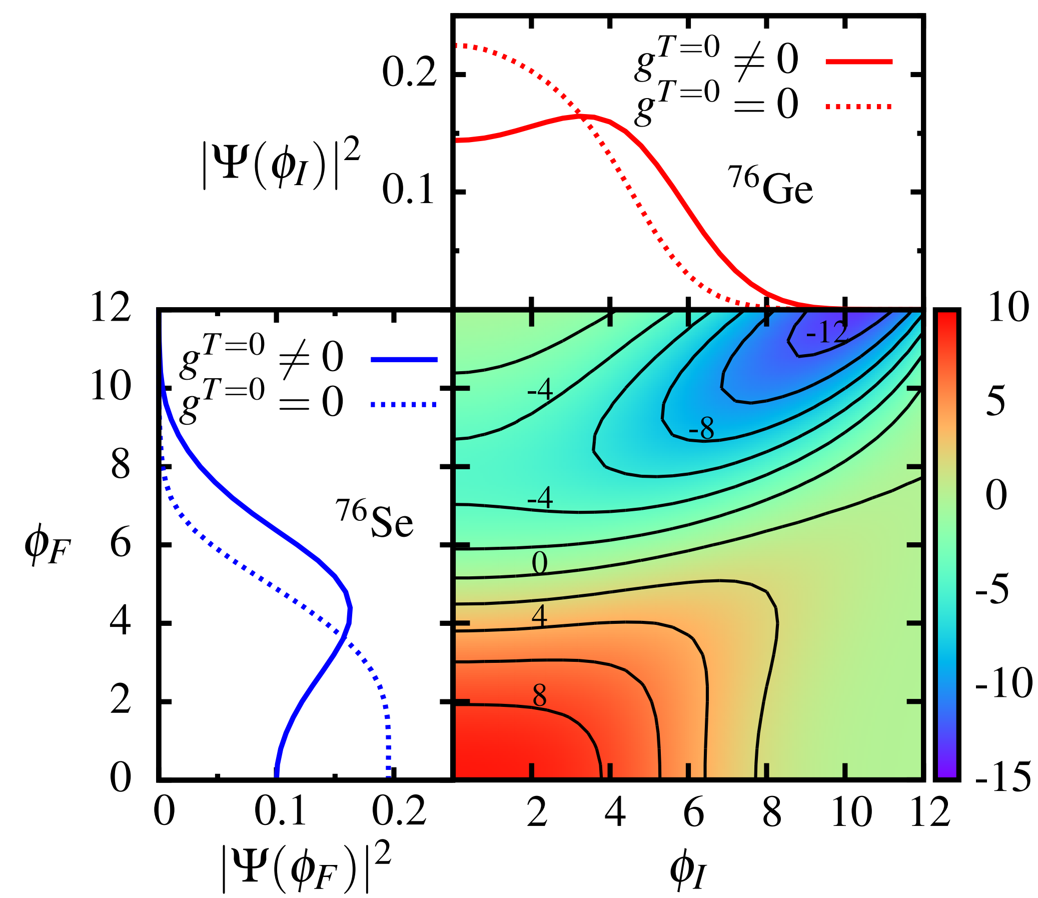

FIG. 3. (Color online.) **Bottom right:** $\mathcal{N}_{\phi_I}\mathcal{N}_{\phi_F}\langle\phi_F|\mathcal{P}_F\hat{M}_{0\nu}\mathcal{P}_I|\phi_I\rangle$ for projected quasiparticle vacua with different values of the initial and final isoscalar pairing amplitudes ϕ_I and ϕ_F, from the SkO′-based interaction (see text). **Top and bottom left:** Square of collective wave functions in ^{76}Ge and ^{76}Se.

N. Hinohara and J. Engel, PRC 031031(R) (2014)

NME: *pf*-shell

Where do the differences between SM and GCM come from?

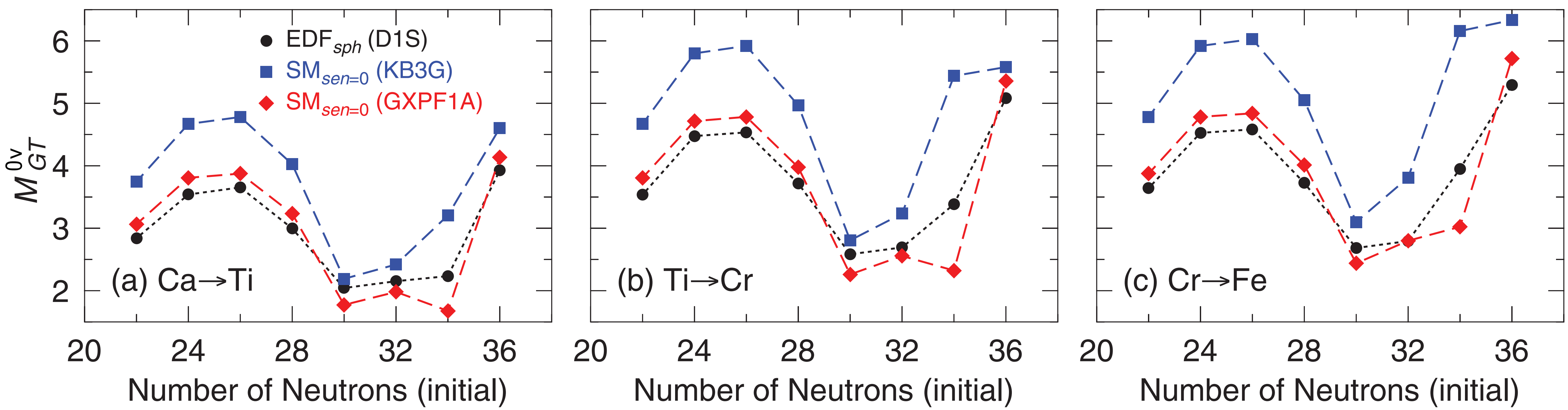

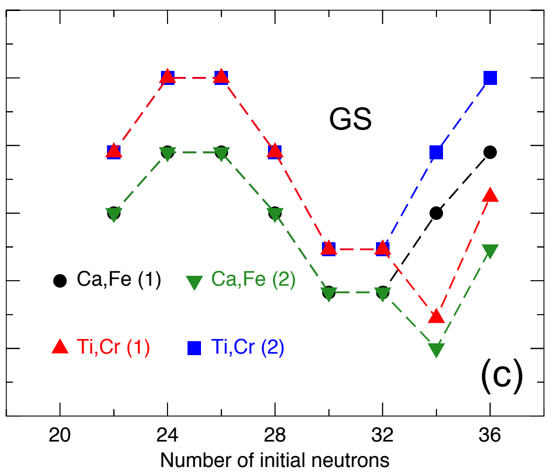

J. Menéndez, T. R. R., A. Poves, G. Martínez-Pinedo, PRC 90, 024311 (2014).

NME: *pf*-shell

Where do the differences between SM and GCM come from?

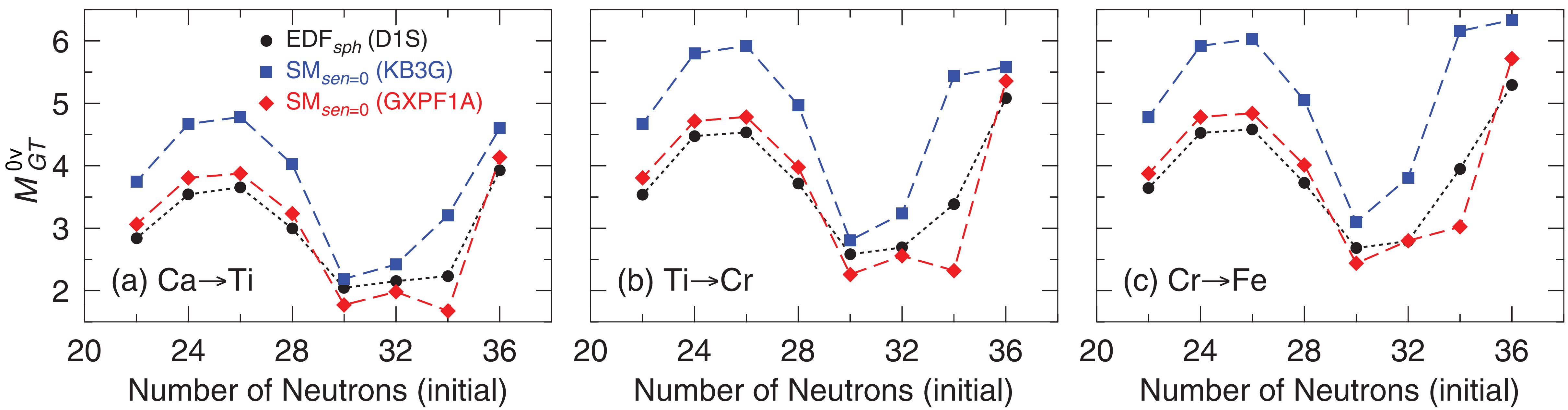

- Same pattern in spherical EDF, seniority 0 Shell Model, and Generalized Seniority model (overall scale?)

- What is the effect of including more **correlations**?

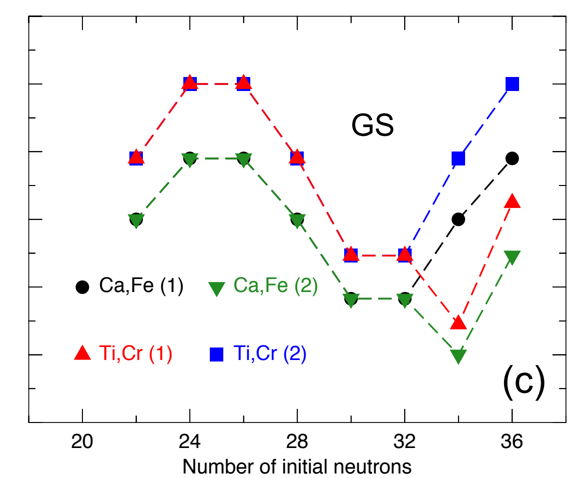

J. Menéndez, T. R. R., A. Poves, G. Martínez-Pinedo, PRC 90, 024311 (2014).

NME: *pf*-shell

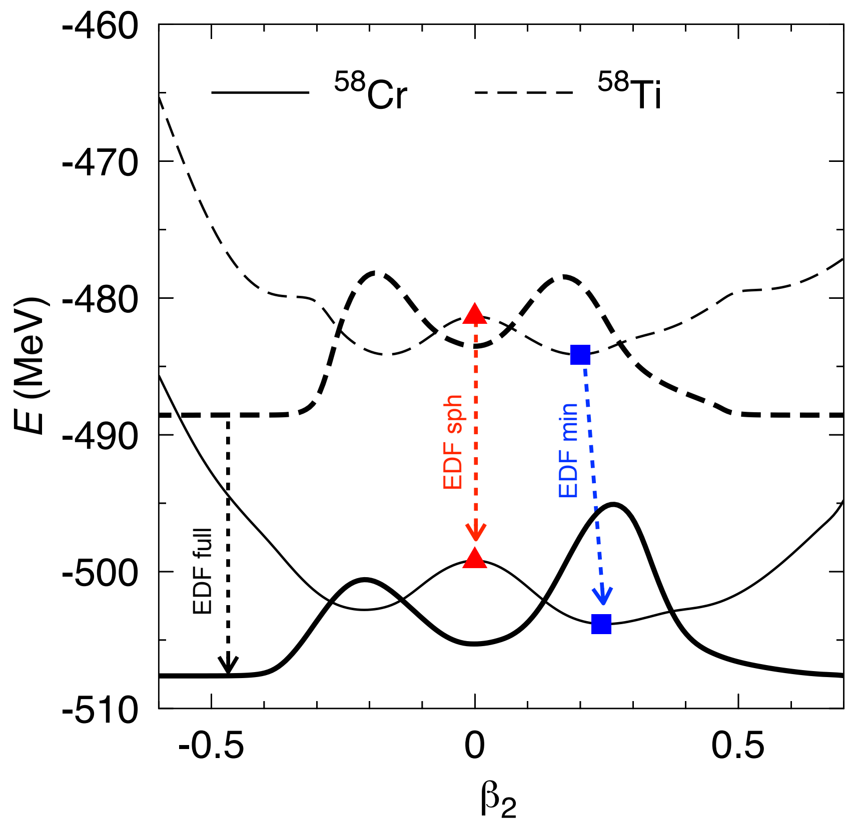

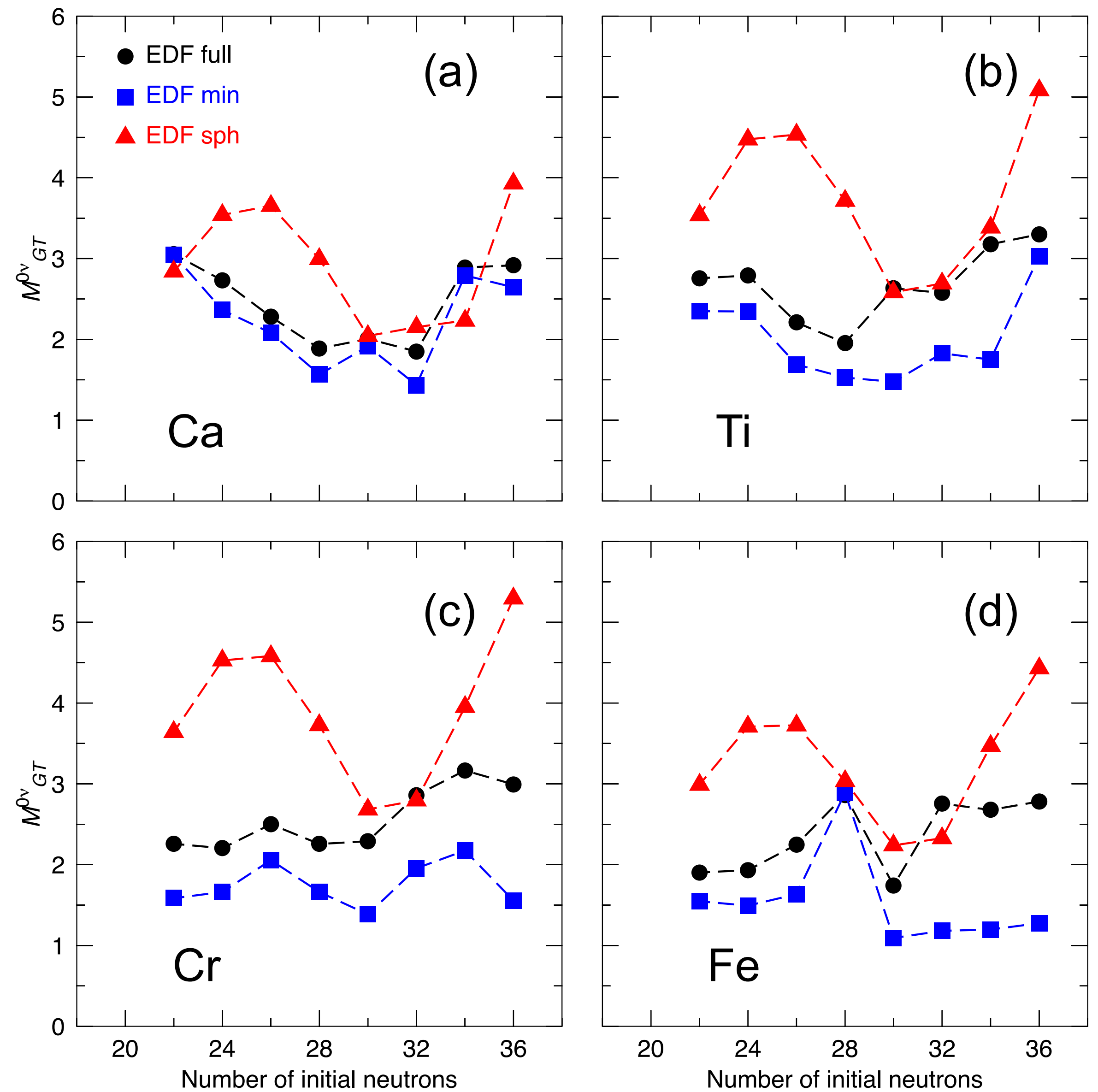

J. Menéndez, T. R. R., A. Poves, G. Martínez-Pinedo, PRC 90, 024311 (2014).

NME: *pf*-shell

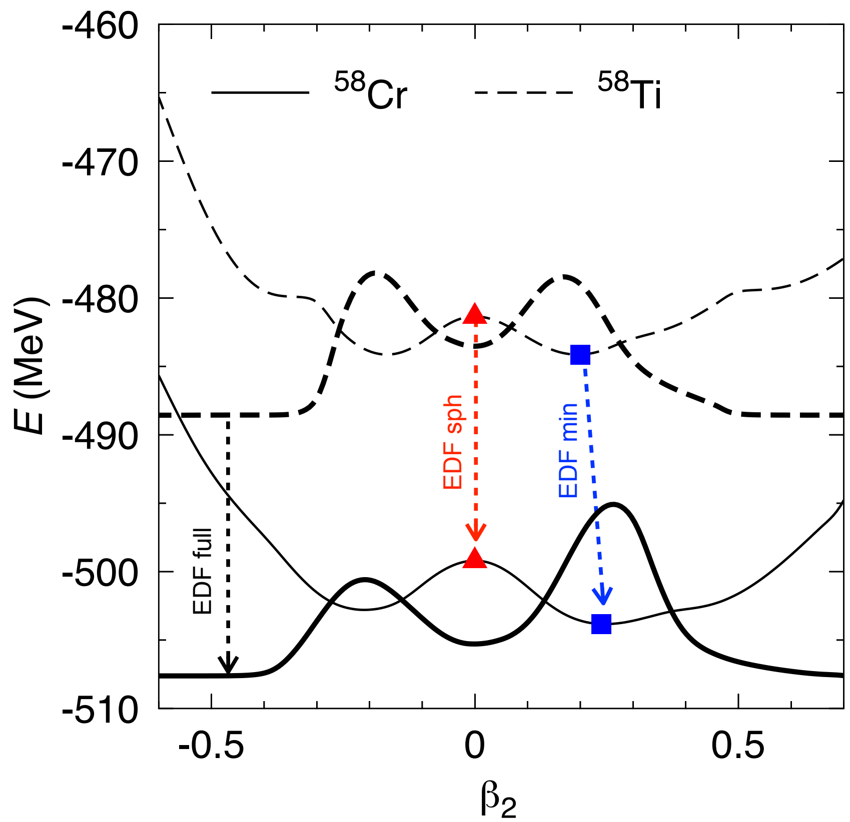

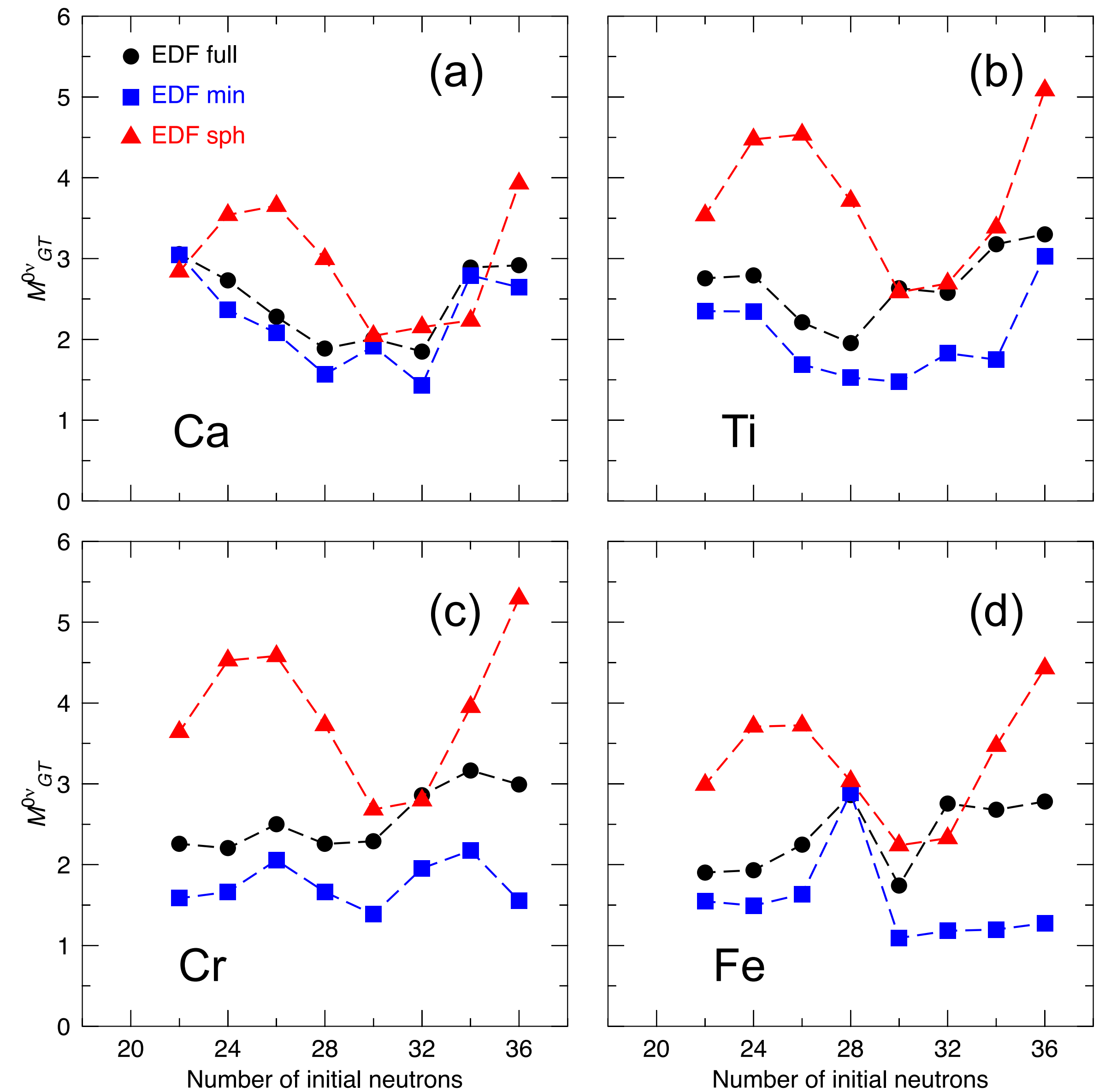

- NMEs are reduced with respect to the spherical value when correlations are included.

- The biggest reduction is produced by angular momentum restoration and configuration mixing produces an increase of the NME.

- Cross-check nuclei: ^{42}Ca, ^{50}Ca, ^{56}Fe

J. Menéndez, T. R. R., A. Poves, G. Martínez-Pinedo, PRC 90, 024311 (2014).

NME: *pf*-shell

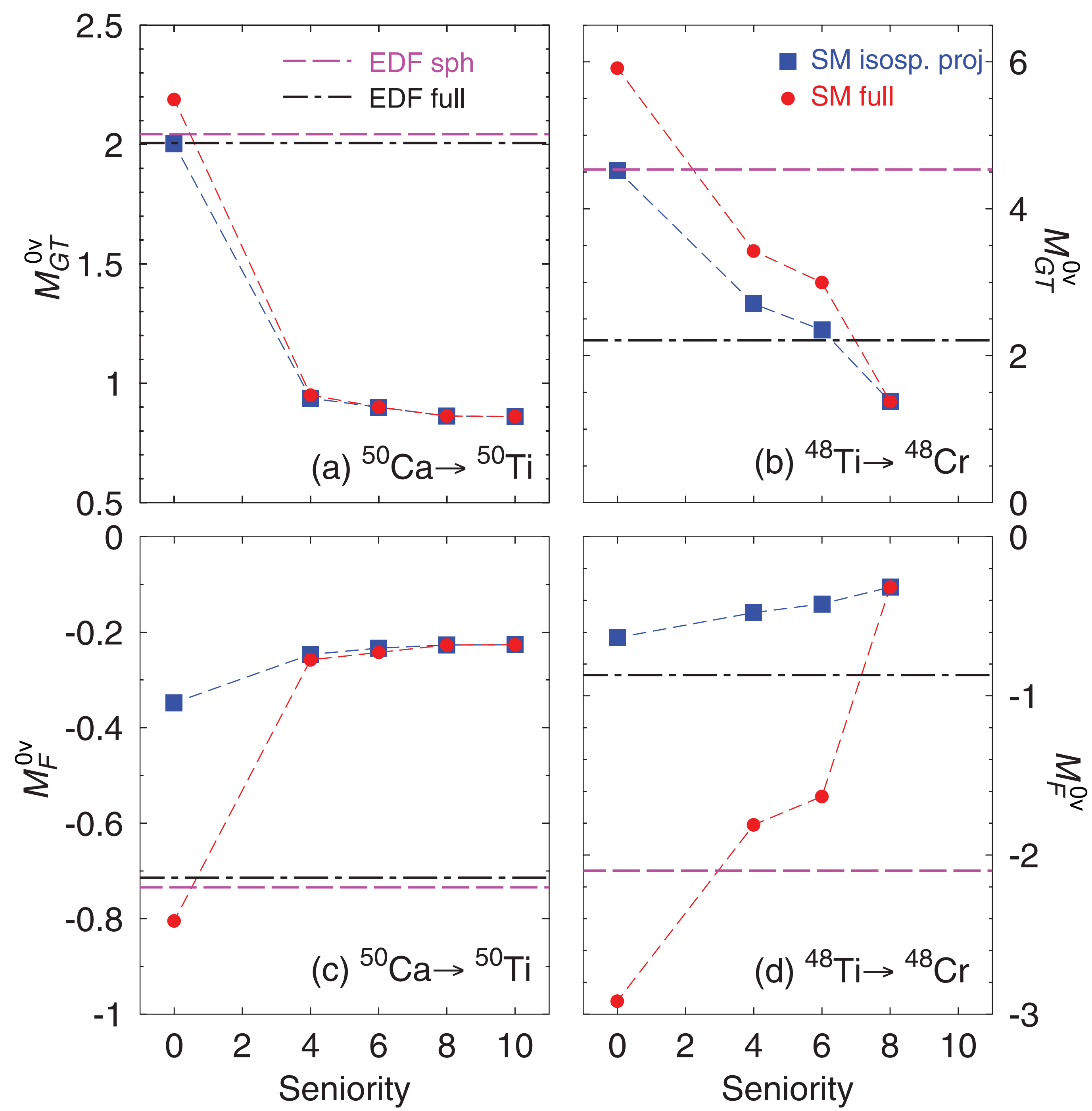

J. Menéndez, T. R. R., A. Poves, G. Martínez-Pinedo, PRC 90, 024311 (2014).

NME: *pf*-shell

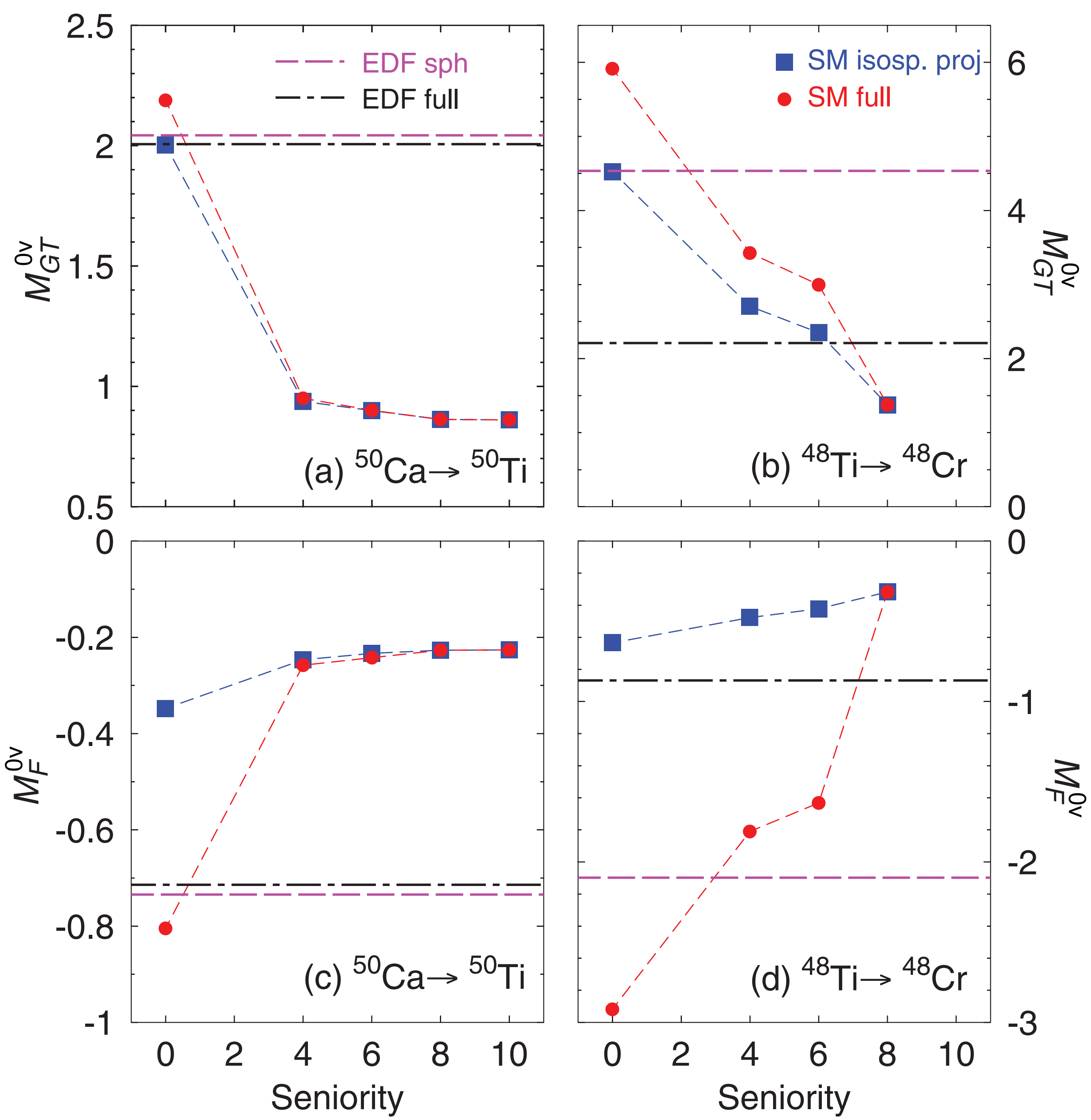

- The biggest reduction (in Shell model calculations) is produced by including higher seniority components in the nuclear wave functions.
- Isospin projection is relevant for the Fermi part of the NME and less important for the Gamow-Teller part.
- EDF does not include properly those higher seniority components, specially in spherical nuclei.
- p-n pairing effects could also be important in the reduction of the NME.

J. Menéndez, T. R. R., A. Poves, G. Martínez-Pinedo, PRC 90, 024311 (2014).

NME: *pf*-shell

J. Menéndez, et al., PRC 93, 014305 (2016).

$$H_{\rm coll} = H_M + g^{T=1}\sum_{n=-1}^{1} S_n^\dagger S_n + g^{T=0}\sum_{m=-1}^{1} P_m^\dagger P_m$$

$$+ g_{ph}\sum_{m,n=-1}^{1} :\mathcal{F}_{mn}^\dagger \mathcal{F}_{mn}: + \chi\sum_{\mu=-2}^{2} :Q_\mu^\dagger Q_\mu:$$

- Increase of the NME when isoscalar pairing is removed.
- Further increase when spin-isospin is also removed

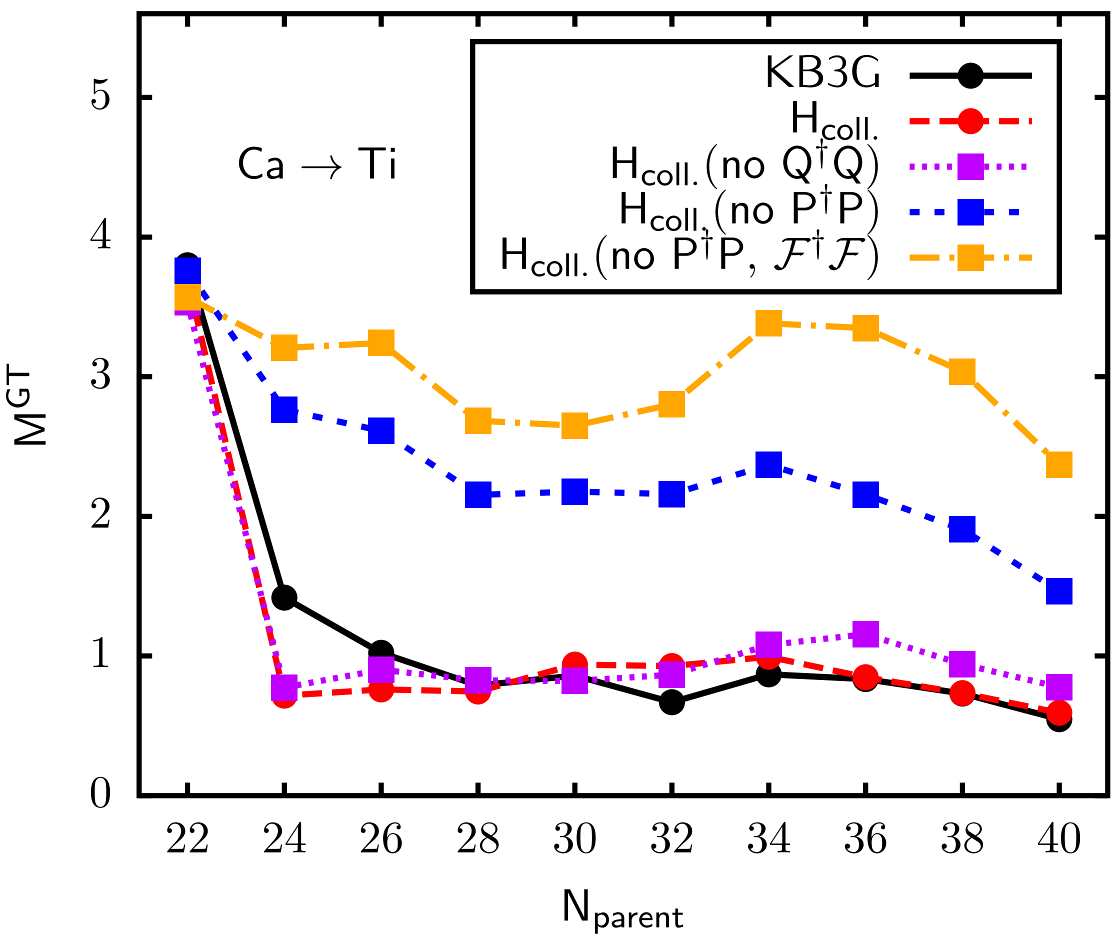

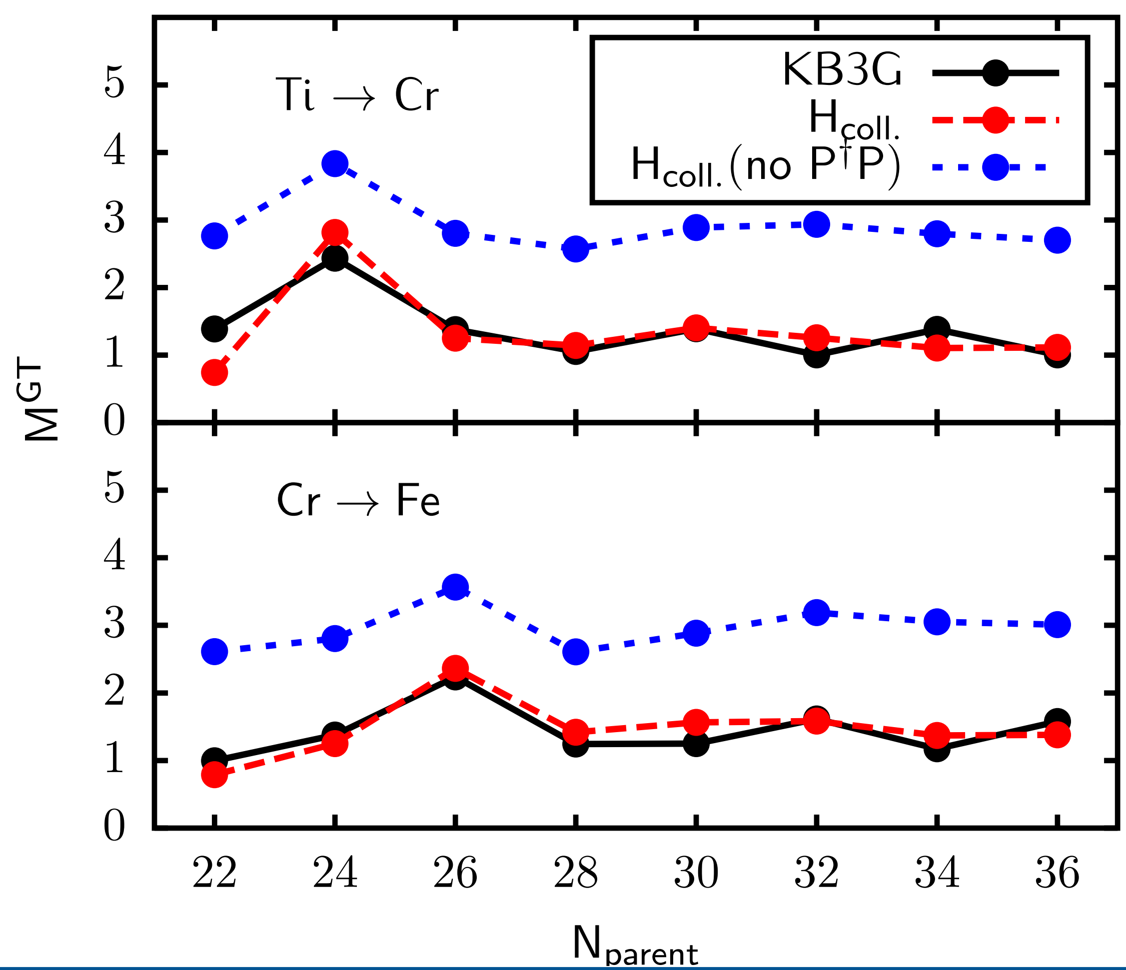

NME: *pf*-shell

J. Menéndez, et al., PRC 93, 014305 (2016).

$$H_{\rm coll} = H_M + g^{T=1}\sum_{n=-1}^{1} S_n^\dagger S_n + g^{T=0}\sum_{m=-1}^{1} P_m^\dagger P_m$$

$$+ g_{ph}\sum_{m,n=-1}^{1} :\mathcal{F}_{mn}^\dagger \mathcal{F}_{mn}: + \chi\sum_{\mu=-2}^{2} :Q_\mu^\dagger Q_\mu:$$

- GT operator is SU(4) invariant (neglecting the neutrino potential)
- GT operator can only connect states belonging to the same irreducible representation of SU(4)
- SU(4) is more broken when T=0 and spin-isospin terms are removed from the Hamiltonian⇒ the number of SU(4) irreps

  present both in the mother and daughter g.s. wave functions are larger⇒ larger NMEs

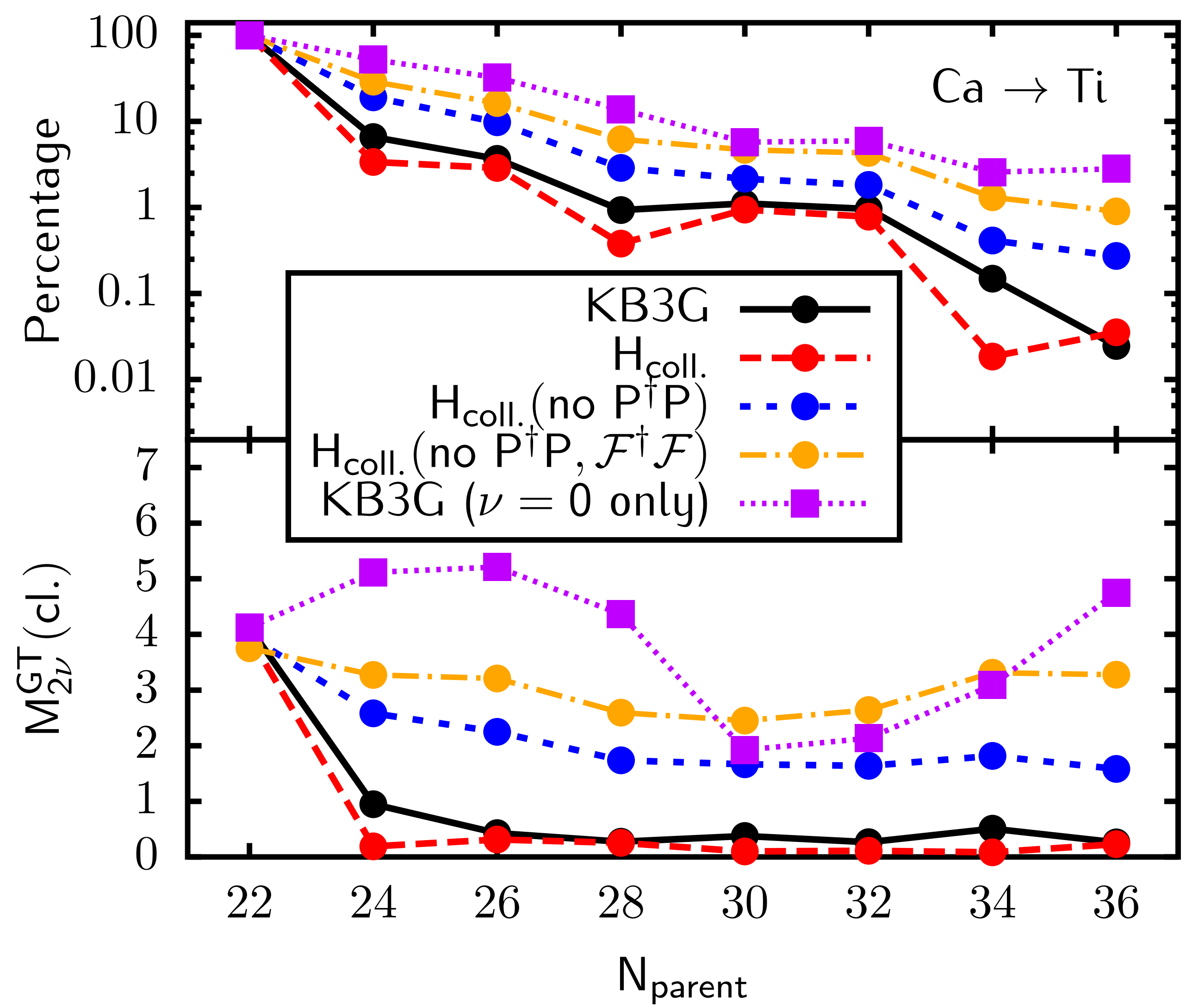

NME: *pf*-shell

J. Menéndez, et al., PRC 93, 014305 (2016).

$$H_{\text{coll}} = H_M + g^{T=1} \sum_{n=-1}^{1} S_n^\dagger S_n + g^{T=0} \sum_{m=-1}^{1} P_m^\dagger P_m$$

$$+ g_{ph} \sum_{m,n=-1}^{1} : \mathcal{F}_{mn}^\dagger \mathcal{F}_{mn} : + \chi \sum_{\mu=-2}^{2} : Q_\mu^\dagger Q_\mu :$$

- SM/GCM comparison with **the same interaction.**

- 1D: only pn strength as a generator coordinate.
- 2D: pn strength and axial quadrupole deformation as generator coordinates.

EXACT vs. VARIATIONAL!!

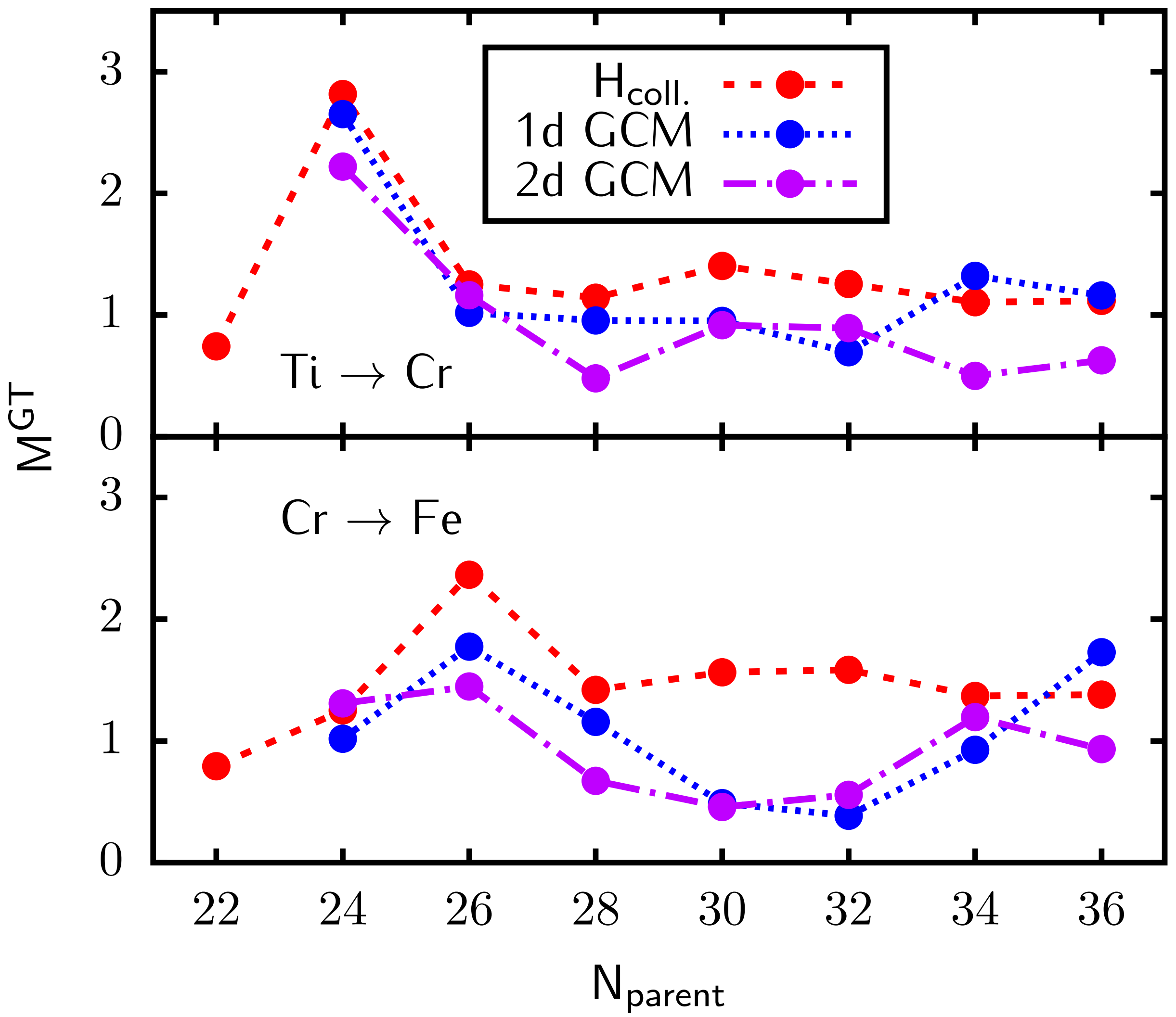

Summary

- NMEs differ a factor of three between the different methods but we need to understand which are the pros/cons of each method to provide reliable numbers (precision vs. accuracy).

- Nuclear physics aspects like deformation, pairing, shell effects, etc., are understood similarly within different approaches.

- Systematic comparisons between ISM/EDF methods have been performed but… we need more!

Open questions

- **Isospin mixing and restoration have to be done in the future. Why is it so difficult (perhaps impossible) with the current Gogny EDFs?**

- **Triaxiality has to be taken into account in *A*=76 and *A*=100 decays (at least).**

- **How relevant is the proper description of the spectra in $0\nu\beta\beta$ NMEs?**

- **Occupation numbers with EDF to define physically sound valence spaces.**

- **Odd-odd nuclei is still a major challenge for GCM calculations.**

- **Computational time?!?**